Effects of nonadiabaticity of collective motion in even–even deformed nuclei

Ph. N. Usmanov and I. N. Mikhaĭlov
Joint Institute for Nuclear Research, Dubna

Fiz. Élem. Chastits At. Yadra **28**, 887–950 (July–August 1997)

A series of methods and nuclear models for describing the properties of the ground and excited positive-parity states of even–even deformed nuclei are described and tested on practical problems. Some models are illustrated by examples of their application. Calculations are carried out for the isotopes ^{164,166,168,170}Er, ^{156,158,160,162,164}Dy, and ^{156}Gd. The experimentally observed properties of low-lying states are studied systematically, and the structure of the wave functions of rotational levels is analyzed. The role of angular $M1$ resonance states in the mixing of states with different internal configurations is discussed. The predictive powers of the methods and models are demonstrated. © *1997 American Institute of Physics.* [S1063-7796(97)00204-0]

INTRODUCTION

The adiabatic model of the nucleus proposed by Bohr and Mottelson, which is a phenomenological model, has played an important role in the study of the properties of deformed nuclei. According to this model, low-lying excited states of even–even deformed nuclei are associated with the rotation of the axially symmetric nucleus as a whole, while higher-lying excited states are viewed as oscillations of the nuclear surface. This simple phenomenological treatment has made it possible to describe a large number of experimental facts pertaining to deformed nuclei and to predict new properties of such nuclei.[1–3]

The advances in experimental nuclear physics associated with improvements in accelerator technology, detection methods, and modernization of data processing have led to the appearance of qualitatively new experimental information about the spectrum, electromagnetic properties, and β-decay characteristics of states in a wide range of angular momenta.[4–9]

There are several general features of the structure of deformed even–even nuclei which have determined how the experimental data are described theoretically. These nuclei possess rather "long" rotational bands. The spectrum of nonrotational states is very rich (expecially for rare-earth and actinide nuclei). Sometimes there are cases where there are several rotational bands with negative and positive parity lying in a very narrow range of excitation energies. These factors create conditions for the mixing of adiabatic states with fixed values of K, the projection of the angular momentum on the nuclear symmetry axis. Actually, the experimental data strongly suggest that there are deviations from the adiabatic theory. The law $E(I)\sim I(I+1)$ is violated with increasing angular momentum I. This may be related both to change of the moment of inertia when the frequency of rotation changes, and to rearrangement of the internal angular momenta of excitations of different origin. The power-series expansion[1]

$$E(I)=AI(I+1)+BI^2(I+1)^2+CI^3(I+1)^3+\cdots,$$

where I is the angular momentum of the state and A, B, and C are phenomenological parameters, has turned out not to be useful for describing the energies of "long" rotational bands of nuclei; it is practically impossible to use it for extrapolating data to large angular momenta. It is very difficult to construct a physical picture leading to deviation from the adiabatic theory at the phenomenological level using parameters like A, B, and C, and the microscopic calculation of these parameters involves various uncertainties.

Expansions of the moment of inertia and the energy in powers of the rotation frequency $\omega_{\rm rot}$ are more successful at reproducing the data on the energies of rotational bands. Using the relation from classical mechanics

$$\frac{\partial}{\partial\omega_{\rm rot}}\left(E(\omega_{\rm rot})-\omega_{\rm rot}\tilde{I}\right)=0$$

between the energies E, the angular momentum $\tilde{I}=\sqrt{I(I+1)}$, and the angular frequency of rotation ($\omega_{\rm rot}=\partial E/\partial\tilde{I}$), we obtain the expression

$$E(I)=\alpha\omega_{\rm rot}^2(I)+\beta\omega_{\rm rot}^4(I)+\gamma\omega_{\rm rot}^6(I)+\cdots, \tag{1}$$

in which the parameters α, β, and γ occur in the expansion of the angular momentum in powers of $\omega_{\rm rot}$:

$$\sqrt{I(I+1)}=2\alpha\omega_{\rm rot}(I)+\frac{4}{3}\beta\omega_{\rm rot}^3(I)+\frac{6}{5}\gamma\omega_{\rm rot}^5(I)+\cdots. \tag{2}$$

This expansion was proposed by Harris[10] on the basis of the Inglis cranking model.[11,12] The convergence of (2) is considerably better than that of (1), so that only two parameters are needed for describing the spin dependence of the energy up to $\sim 10\hbar$. According to Ref. 12, Eqs. (1) and (2) allow the energy spectra to be reproduced also at higher spins. However, this description of the spectrum of rotational bands also has its limitations, which are especially clear in describing rotational bands constructed on states with internal excitation.

Study of the spectra of rotational bands clearly suggests that nonadiabatic effects cannot always be described in first-order perturbation theory in the parameters of the Coriolis mixing of states. Significant deviations from the predictions

 1063-7796/97/040348-26$10.00 © 1997 American Institute of Physics

of the adiabatic theory are observed in the energy spectrum of rotational bands of excited states and in the branching of electromagnetic transitions between states of rotational bands. The predictions of the adiabatic theory often differ from the experimental data by hundreds of percent or even an order of magnitude. As a rule, these deviations also cannot be described in the lowest orders of perturbation theory in the parameters of the Coriolis band coupling. For example, the Mikhaĭlov expression,[13] obtained for describing deviations from the rules for the intensities of $E2$ transitions between interacting $K^\pi=0^+$ and $K^\pi=2^+$ bands [taking into account terms of first order in the expansion of the energy in $I(I+1)$]

$$B(E2;K=2I_i\to K=0I_f)=2M_i^2\{C^{I_f0}_{I_i2;2-2}[1+a_2[I_f(I_f+1)-I_i(I_i+1)]]^2, \quad (3)$$

in many cases cannot reproduce the experimental data.[14–20]

Therefore, it is very important to look for phenomenological and microscopic approaches which can be used to describe the spectral and decay characteristics of states in a wide range of excitation energies and angular momenta.

For intermediate values of the spin, nonadiabatic effects can be described by models in which the mixing of a limited number of states of relatively low excitation energy is taken into account. The coupling of collective bands in such models has been taken into account by many authors. However, in many cases only the lower part of the energy spectrum and an insufficient number of rotational bands participating in the mixing were taken into account.

The study of the properties of deformed nuclei has become particularly interesting in recent years in connection with the discovery of a new collective isovector magnetic dipole mode. The measured values of the excited-state energies of such modes indicate that they do not lie very high in the excitation spectrum, and the inclusion of the mixing of states of isovector magnetic modes with low-lying states can lead to interesting physical phenomena.

In this review we describe several methods and nuclear models designed to study deviations from the adiabatic theory manifested in the energies and electromagnetic characteristics of excited states of even–even deformed nuclei. We systematically study the experimentally observed properties of low-lying states, and analyze the structure of the wave functions of the rotational levels. The role of states of the angular $M1$ resonance in the mixing of states with different internal configurations in radionuclides of the deformed region is discussed.

1. A PHENOMENOLOGICAL MODEL FOR STUDYING THE PROPERTIES OF POSITIVE-PARITY STATES

Nonadiabatic effects indicate the presence of coupling between the rotational motion and internal excitations in nuclei. The use of phenomenological models makes it possible to determine the most important elements of this coupling and to interpret sometimes unexpected effects.

In constructing such models, it is important to choose appropriately the space of states whose mixing can explain the observed phenomena. This involves several considerations.

It is known that, as a rule, in even–even nuclei the moment of inertia of the ground-state (gr) band is smaller than the moments of inertia of the β- and γ-vibrational bands ($\mathscr{T}_{gr}<\mathscr{T}_\beta$, $\mathscr{T}_\gamma$). This relation between the energy ranges cannot be reproduced when the deviations from the rigid-rotor model are viewed as the result of direct rotational mixing of the gr, β, and γ bands. However, it can be explained in a model which includes Coriolis coupling of the states of the gr, β, and γ with higher-lying bands.

In experiments on electron and photon scattering on many nuclei of the deformed region,[21–28] collective $K^\pi=1^+$ states have been discovered which have strong $M1$ transitions to the ground state. These excitation modes have been described using various approaches.[29–40] Several states with $I^\pi=1^+$ and the corresponding values of $B(M1)$ have also been found[27,28] in an experiment on photon scattering on the isotopes ^{160,162,164}Dy, ^{172,174,176}Yb, and ^{156}Gd. The ratios of the reduced $M1$-transition probabilities $R=B(M1;1^+1\to 2^+0_{gr})/B(M1;1^+1\to 0^+0_{gr})$ from these levels agree with the adiabatic values calculated using the Alaga rule and allow the quantum numbers $K^\pi=1^+$ to be assigned to these bands. Accordingly, it is interesting to study the effect of $K^\pi=1^+$ states on the properties of low-lying levels. In this situation it is thought that the larger (than in the ground-state band) effective moments of inertia of the β and γ bands arise because the mixing of these bands with the $K^\pi=1^+$ band is more intense than the mixing between the gr and $K^\pi=1^+$ bands. Important effects due to the coupling of the β, γ, and $K^\pi=1^+$ bands can be expected when the ground-state energies of the β and γ rotational bands are close to each other.

In this section we shall analyze a phenomenological model for studying the properties of positive-parity states which includes the Coriolis mixing of states of the gr, β, γ, and $K^\pi=1^+$ bands. Calculations are performed for the isotopes ^{164,166,168,170}Er, ^{156,158,160,162,164}Dy, and ^{156}Gd. The energy spectra are described. The reduced probabilities of quadrupole and monopole electric transitions between states of the rotational bands are calculated. The nonadiabatic features manifested in electromagnetic transitions are discussed, as well as the behavior of the Rasmussen parameter $X_I^{if}=B(E0;I0_i^+\to I0_f^+)/B(E2;I0_i^+\to I0_f^+)$ between levels of nonzero spin. The values of the dimensionless nuclear matrix element of the $E0$ transition, $\rho(E0)$, are estimated. In particular, the effect of states of the $K^\pi=1^+$ band on the electromagnetic characteristics of low-lying levels is studied. The difference of the g_R factors of states of the ground and γ bands for low spins is explained. The values of the multipole-mixture coefficients δ calculated for $\gamma\to\gamma$, $\gamma\to$ gr, and $\beta\to$ gr transitions are compared with the experimental data.

1.1. Formulation of the model

We shall consider deformed nuclei in which well localized principal axes are distinguished (an internal coordinate system). The spatial orientation of the system is determined

by the Euler angles θ_i. In the generalized model of the nucleus it is assumed that the complete nuclear Hamiltonian consists of two parts:

$$H=H(R^2)+H_{\rm int},$$

$$\mathrm{H}_{\rm int}=\sum_K \omega_K \mathbf{b}_K^+ \mathbf{b}_K, \tag{1.1}$$

where $H(R^2)$ describes the rotational energy of the nucleus and is a function of the rotational angular momentum R ($R=I-j$, where I is the total and j is the internal angular momentum). The second term is the internal part of the Hamiltonian, which we write out by introducing phonon operators $\mathbf{b}_K^+$ ($\mathbf{b}_K$) which create (annihilate) excited states of positive parity, and ω_K are the values of the principal band energies.

An eigenfunction of the Hamiltonian has the form

$$|IMK\rangle=\sqrt{\frac{2I+1}{16\pi^2}}\left\{\sqrt{2}\psi^I_{\rm gr,K}D^I_{M,0}(\theta)\right.$$
$$+\sum_{K'}\frac{\psi^I_{K',K}}{\sqrt{1+\delta_{K',0}}}[D^I_{M,K'}(\theta)b^+_{K'}$$
$$\left.+(-1)^{I+K'}D^I_{M,-K'}(\theta)b^+_{-K'}]\right\}|0\rangle. \tag{1.2}$$

Here $\psi^I_{K',K}$ are the mixing amplitudes of the basis states. The space of states consists of $(3+l)$ bands, where l is the number of included 1^+ states. It also contains the ground-state band $|0\rangle$, the one-phonon bands $\mathbf{b}^+_{\lambda=2,K}|0\rangle=\mathbf{b}^+_K|0\rangle$ with $K^\pi=0^+_\beta$, 2^+, and the 1^+_l bands.

The Hamiltonian (1.1) possesses transformation properties such that the state (1.2) can be classified by a quantum number, the signature $\sigma=\pm1$, which imposes constraints on the values of the angular momentum $(-1)^I\sigma=1$. This leads to a significant difference in the mixing of states with different signature.

We shall write the rotational part of the Hamiltonian $H(R^2)$ as a Taylor expansion in powers of j. Keeping only the zeroth- and first-order terms, we obtain the Hamiltonian

$$H=H_{\rm rot}(I^2)+H^\sigma_{K,K'}(I), \tag{1.3}$$

$$H^\sigma_{K,K'}(I)=\omega_K\delta_{K,K'}-\omega_{\rm rot}(I)(j_x)_{K,K'}\cdot\chi(I,K)\delta_{K',K\pm1}, \tag{1.4}$$

acting in the space of states (1.2) with fixed values of the angular momentum I. In Eq. (1.4), $\omega_{\rm rot}(I)=dE_{\rm core}(I)/dI$ is the angular rotation frequency of the core $[E_{\rm core}(I)\equiv H_{\rm rot}(I(I+1))]$, j_x is the projection of the internal angular momentum on the x axis, and

$$\chi(I,0)=1,\quad \chi(I,1)=\left[1-\frac{2}{I(I+1)}\right]^{1/2},$$
$$(j_x)_{\rm gr,1}=-\sqrt{3}\cdot\eta_0,\quad (j_x)_{\beta,1}=-\sqrt{3}\cdot\eta_1, \tag{1.5}$$
$$(j_x)_{\gamma,1}=-1\cdot\eta_2.$$

By solving the Schrödinger equation

$$(H^\sigma_{K,\nu}(I)-\varepsilon^\sigma_\nu)\psi^\sigma_{K,\nu}=0, \tag{1.6}$$

we find the eigenfunctions and energies of the positive-parity states.

The total energy of a state is given by

$$E^\sigma_\nu(I)=E_{\rm core}(I)+\varepsilon^\sigma_\nu(I). \tag{1.7}$$

The energy of the rotating core $E_{\rm core}(I)$ can be determined by various methods, for example, by the Harris parametrization for the energy and angular momentum[10] [Eq. (1)].

1.2. Electric quadrupole transitions

We shall calculate the reduced probability for $E2$ transitions[1,2]

$$B(E2;I_iK_i\to I_fK_f)=\frac{1}{2I_i+1}|\langle I_fK_f||m(E2;\mu)||I_iK_i\rangle|^2 \tag{1.8}$$

between states of the type (1.2).

The components of the electric quadrupole tensor in the laboratory frame are related to the components in the internal frame by the standard transformation

$$\hat m(E2;\mu)=\sqrt{\frac{5}{16\pi}}eQ_0D^2_{\mu,0}(\theta)$$
$$+\sum_\nu \hat m'(E2;\nu)D^2_{\mu,\nu}(\theta), \tag{1.9}$$

where

$$\hat m'(E2;\nu)=m_\nu(b^+_\nu+(-1)^\nu b_{-\nu}).$$

Here Q_0 is the internal quadrupole moment of the nucleus, and m_ν are constants determined from the experimental values of $B(E2)$.

The reduced probability of $E2$ transitions from one-phonon states $|I_iK_ib_i\rangle$ to levels of the ground-state band is

$$B(E2;I_iK_i\to I_f{\rm gr})=\left\{\sqrt{\frac{5}{16\pi}}eQ_0\left[\psi^{I_f}_{\rm gr,gr}\psi^{I_i}_{{\rm gr},K_i}C^{I_f0}_{I_i0;20}\right.\right.$$
$$\left.+\sum_n \psi^{I_f}_{K_n,{\rm gr}}\psi^{I_i}_{K_n,K_i}C^{I_fK_n}_{I_iK_n;20}\right]$$
$$+\sqrt{2}\left[\psi^{I_f}_{\rm gr,gr}\sum_n\frac{(-)^{K_n}m_{K_n}\psi^{I_i}_{K_n,K_i}}{\sqrt{1+\delta_{K_n,0}}}\right.$$
$$\times C^{I_f0}_{I_iK_n;2-K_n}+\psi^{I_i}_{{\rm gr},K_i}$$
$$\left.\left.\times\sum_n\frac{m_{K_n}\psi^{I_f}_{K_n,{\rm gr}}}{\sqrt{1+\delta_{K_n,0}}}C^{I_fK_n}_{I_i0;2K_n}\right]\right\}^2, \tag{1.10}$$

where

$$m_K=\langle{\rm gr}|\hat m(E2)|K^\pi\rangle,\quad K^\pi=0^+,2^+\ \text{and}\ 1^+_\nu.$$

In the adiabatic approximation, the reduced probabilities of $E2$ transitions from the β and γ vibrational bands are

$$B^{\rm rot}(E2;I_i\beta\to I_f{\rm gr})=|m_0C^{I_f0}_{I_i0;20}|^2, \tag{1.11}$$

$$B^{\rm rot}(E2;I_1\gamma\to I_f{\rm gr})=2|m_2C^{I_f0}_{I_i2;2-2}|^2, \tag{1.12}$$

which allows the values of the parameters m_0 and m_2 to be calculated from experiment. However, when the β and γ bands lie close together, they are strongly mixed even for $I=2$, and the adiabatic approximation (1.11) and (1.12) becomes inapplicable (for example, for the nucleus ^{232}Th).[15]

For the reduced probabilities of $E2$ transitions from states of the γ band with $\sigma=-1$ (I-odd states), Eq. (1.10) takes the form

$$B(E2;I_i\gamma\to I_f0_{gr})$$
$$=\left\{\sqrt{\frac{5}{16\pi}}Q_0\sum_{K=1}\psi^{I_f}_{K,{\rm gr}}\psi^{I_i}_{K,\gamma}C^{I_fK}_{I_iK;20}+\sqrt{2}\psi^{I_f}_{{\rm gr,gr}}\right.$$
$$\left.\times\sum_{K=1}(-1)^Km_K\psi^{I_i}_{K,\gamma}C^{I_f0}_{I_iK;2-K}\right\}^2. \tag{1.13}$$

This expression can be used to find m_1 if the experimental values of $B(E2)$ or the ratios of the reduced $E2$-transition probabilities $R_{I\gamma}=B(E2;I_\gamma\to(I+1)_{\rm gr})/B(E2;I_\gamma\to(I-1)_{\rm gr})$ are known. The deviation of the ratio $B(E2)/B^{\rm rot}(E2)$ from 1 determines the degree of nonadiabaticity of $E2$ transitions.

1.3. Electric monopole transitions

Electromagnetic transitions are extremely important for understanding and analyzing the various nuclear excitation modes. Electric monopole transitions play a special role here. They are associated with interesting and little-studied aspects of nuclear structure like changes in the rms radii, the compressibility of nuclear matter, radial density oscillations, the breathing mode, and so on.[41]

The main factor producing $E0$ transitions is the Coulomb interaction of the intranuclear nucleons with the electrons of the atomic shell. Other electromagnetic interactions and other interactions in general usually are not involved.[42] One-photon $E0$ transitions are strictly forbidden by angular-momentum conservation.

As a rule, monopole transitions are accompanied by more intense quadrupole ones. In those cases where the lifetime of the studied level cannot be determined, the value of the $E0/E2$ mixing is measured:[43]

$$X_I(E0/E2)=\frac{B(E0;i\to f)}{B(E2;i\to f')}=\frac{e^2R_0^4\rho^2(E0;i\to f)}{B(E2;i\to f')}, \tag{1.14}$$

where ρ is the dimensionless matrix element of the $E0$ transition and $R_0=r_0A^{1/3}$ is the nuclear charge radius. The states i and f must have identical spin and parity. Transitions between monopole states are compared with $E2$ transitions from a given 0^+ level to the 2^+ level closest to the final state. The experimental information about the transition is often limited to just this one parameter. On the other hand, since the ratio $X(E0/E2)$ is independent of electron factors and transition energies, it is useful for comparison with nuclear models.

The model described above gives the following expression for the reduced probabilities of $E0$ transitions from states of the $K^\pi=0^+_\nu$ band to levels of the ground-state rotational band:

$$B(E0;I0_\nu\to I{\rm gr})=\left\{\sum_\nu m'_{0_\nu}(\psi^I_{0_\nu0_2}\psi^I_{{\rm gr,gr}}\right.$$
$$\left.+\psi^I_{{\rm gr},0_2}\psi^I_{0_\nu{\rm gr}})\right\}^2, \tag{1.15}$$

where ν is the number of 0^+ bands included in the basis states of the Hamiltonian (1.3), and $m'_{0_\nu}=\langle{\rm gr}|m(E0)|0^+_\nu\rangle$ are the matrix elements between the internal wave functions of the ground and 0^+_ν bands. These are numerical parameters and are determined experimentally. In our model for the adiabatic case Eq. (1.14) has the form

$$X_I(E0/E2)=X_0(E0/E2)\frac{(2I-1)(2I+3)}{I(I+1)}, \tag{1.16}$$

where

$$X_0(E0/E2)=\frac{B(E0;00_\nu\to0{\rm gr})}{B(E2;00_\nu\to2{\rm gr})}=\left[\frac{m'_{0_\nu}}{m_{0_\nu}}\right]^2. \tag{1.17}$$

Using the experimental values $X_0^{\rm exp}(E0/E2)$ for transitions from 0^+_ν levels, Eq. (1.17) can be used to find the numerical values of the matrix elements m'_{0_ν}. The numerical values of the parameters m_{0_ν} are found from the adiabatic expression (1.11). The determination of the parameters m'_0 using (1.17) is sufficiently accurate, because the 0^+_ν levels are not perturbed by the Coriolis forces.

1.4. The magnetic moment and $M1$ transitions

The dipole magnetic moment of a nucleus in the state (1.2) is given by[1]

$$\mu=\langle IM=IK|\mu_z|IM=IK\rangle,$$

where the z component of the magnetic-moment operator is related to the $M1$-transition operator as

$$\mu_z=\frac{2Mc}{e\hbar}\sqrt{\frac{4\pi}{3}}\,.\hat{\mathscr{M}}\ (M1;\mu=0).$$

The $M1$-transition operator in the internal frame consists of two terms:[1]

$$.\hat{\mathscr{M}}\ (M1;\mu=0)=\sum_\nu\hat m(M1;\nu)D^1_{\mu=0,\nu}$$
$$+\sqrt{\frac{3}{4\pi}}\left(\frac{e\hbar}{2Mc}\right)g_R(I_{\mu=0}-I_3D^1_{\mu=0,0}), \tag{1.18}$$

the first of which gives the contribution of the internal motion, while the second gives the contribution of the rotational

TABLE I. Parameters used in the calculations for Er isotopes.

A	ω_β	ω_1	ω_γ	η_0	η_1	η_2	$\mathcal{J}_0$	$\mathcal{J}_1$
164	1.246	3.0	0.777	0.28	1.95	1.50	31.4	118.4
166	1.460	3.0	0.710	0.62	1.69	2.05	35.3	181.2
168	1.217	3.0	0.732	0.0	2.04	1.10	35.9	111.3
170	0.891	3.0	0.845	0.03	1.29	0.0	36.5	117.8

ω_ν are the parameters of the principal band energies (MeV); η_K is the coefficient of the Coriolis interaction; $\mathcal{J}_0$ and $\mathcal{J}_1$ are the inertia parameters ($\hbar^2$/MeV, $\hbar^4$/MeV^3).

motion to the magnetic moment, which is proportional to the component of the angular momentum perpendicular to the symmetry axis.

Using the common notation

$$\langle K|\hat{m}(M1;\nu=0)|K\rangle=\sqrt{3/4\pi}\left(\frac{e\hbar}{2Mc}\right)g_K K, \tag{1.19}$$

where g_K is the internal g factor of the band with $K\neq 0$, we obtain an expression for the magnetic moment of the K band:

$$\mu_{IK}=g_R I+\sum_{K'=1}|\psi^I_{K,K'}|^2(g_{K'}-g_R)\frac{K'}{I+1}. \tag{1.20}$$

In deriving (1.20) we restricted ourselves to only the diagonal matrix elements (1.19).

In the adiabatic approximation we have:

for the $K^\pi=0^+$ bands (gr and β), $\mu_I=g_R I$;

for the $K^\pi\neq 0^+$ bands (γ and $K^\pi=1^+$),

$$\mu_{IK}=g_R I+(g_K-g_R)\frac{K^2}{I+1}.$$

The systematics of the g_R factors of deformed nuclei of the rare-earth and transuranium regions give $g_R\simeq 0.4\pm 0.1$ ($g_R=Z/A$) (Refs. 1 and 2).

The probability of an $M1$ transition from one-phonon states to levels of the ground-state rotational band is given by

$$B(M1;IK\to I'0_{\rm gr})=\frac{3}{4\pi}\left(\frac{e\hbar}{2Mc}\right)^2\left|\sum_{K_1=1}^{2}\psi^I_{K_1,K}\psi^{I'}_{K_1,{\rm gr}}K_1\right.$$
$$\left.\times C^{I'K_1}_{IK_1;10}(g_{K_1}-g_R)\right|^2. \tag{1.21}$$

According to (1.21), in the adiabatic approximation $M1$ transitions from states of the γ band to levels of the ground-state band are forbidden, i.e., such transitions are possible owing to the Coriolis mixing of states with $\Delta K=1$. In reactions of electron and photon scattering on nuclei, low-lying collective $K^\pi=1^+$ states with a fairly large value of $B(M1;1^+\to 0^+_{\rm gr})$ have been found[21-28] in several nuclei of the rare-earth and transuranium regions. These transitions occur between the principal levels of the $K^\pi=1^+$ and $K^\pi=0^+_{\rm gr}$ bands, which are not perturbed by the Coriolis forces. We describe these transitions in our model by including in the internal magnetic dipole-moment operator an additional term which changes the number of phonons by unity:

$$\hat{m}(M1;\nu)=\sqrt{\frac{3}{4\pi}}\left(\frac{e\hbar}{2Mc}\right)[\hat{m}_{K\nu=0}(b_K b^+_K+b^+_K b_K)\delta_{\nu,0}$$
$$+\hat{m}'_\nu(b(b^+b)^1_K)^1_\nu+\text{H.c.}]. \tag{1.22}$$

The operator (1.22) leads to an additional term in (1.21):

$$B(M1;IK\to I'0_{\rm gr})=\frac{3}{4\pi}\left|\sum_{K_1=1}^{2}\psi^I_{K_1,K}\psi^{I'}_{K_1,{\rm gr}}\right.$$

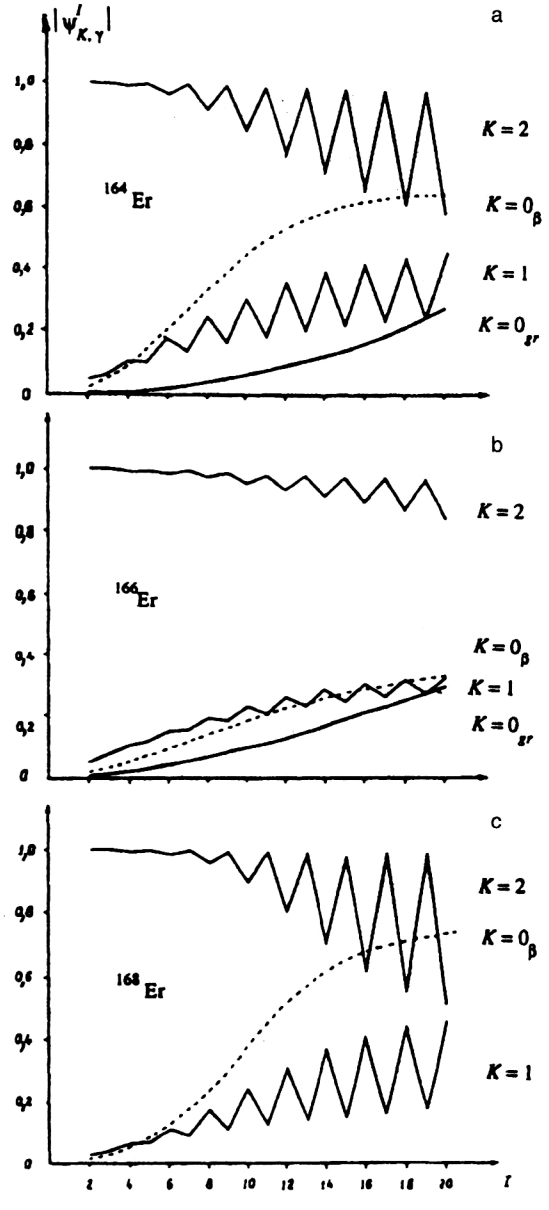

FIG. 1. Structure of the wave functions of states of the γ band for ^{164}Er (a), ^{166}Er (b), and ^{168}Er (c).

TABLE II. Ratios of reduced $E2$-transition probabilities in ^{164}Er.

	Experiment		Theory		
$(I_\gamma \to I'_{gr})/(I_\gamma \to I''_{gr})$	Ref. 46	Ref. 17	Phen. Ref. 14	TRM Ref. 77	Alaga
$(2_\gamma \to 2_{gr})/(2_\gamma \to 0_{gr})$	2.23(14)	1.97(30)	1.86	1.97	1.43
$(2_\gamma \to 4_{gr})/(2_\gamma \to 2_{gr})$	0.11(5)	0.15(3)	0.09	0.09	0.05
$(3_\gamma \to 4_{gr})/(3_\gamma \to 2_{gr})$	0.89(7)	0.82(20)	0.69	0.81	0.40
$(4_\gamma \to 4_{gr})/(4_\gamma \to 2_{gr})$	13.3(19)	5.4(13)	6.1	7.1	2.94
$(5_\gamma \to 6_{gr})/(5_\gamma \to 4_{gr})$	1.45(13)	1.3(3)	1.3	1.8	0.57
$(2_\gamma \to 4_{gr})/(2_\gamma \to 0_{gr})$	0.25(10)	0.36(6)	0.17	0.18	0.075

$$\times K_1 C^{I'K}_{IK_1;10}\cdot(g_{K_1}-g_R)+\frac{\sqrt{6}}{10}\,m'_1\psi^{I'}_{gr,gr}$$

$$\times\psi^{I}_{1,K}C^{I'0}_{I1;11}\Big|^2\left(\frac{e\hbar}{2Mc}\right)^2. \qquad (1.23)$$

In the adiabatic approximation we have

$$B(M1;11^+\to 00^+_{gr})=\frac{3}{4\pi}\left(\frac{e\hbar}{2Mc}\right)^2\cdot 0.02(m'_1)^2. \qquad (1.24)$$

The value of m'_1 can be calculated from the experimental value of the probability for such $M1$ transitions.

The magnetic moment of the state is given by

$$\mu_K(I)=g_R I+\sum_{K'=1}|\psi^I_{K',K}|^2(g_{K'}-g_R)\,\frac{K'^2}{I+1}$$

$$+\frac{\sqrt{3}}{10}\,m'_1\psi^I_{gr,K}\psi^I_{1,K}\sqrt{\frac{I}{I+1}}. \qquad (1.25)$$

Instead of the reduced $M1$-transition probabilities, the multipole-mixture coefficients δ are usually studied. Their values are found experimentally using the expression

$$\delta(I_iK_i\to I_fK_f)=0.834$$

$$\times E_\gamma(\mathrm{MeV})\,\frac{\langle I_fK_f\|\hat m(E2)\|I_iK_i\rangle}{\langle I_fK_f\|\hat m(M1)\|I_iK_i\rangle}\,\frac{e\cdot\mathrm{b}}{\mu_n}. \qquad (1.26)$$

In the adiabatic approximation for (1.26) within a single band with $K\neq 0$ we have

$$\delta=0.933\,\frac{eQ_0}{g_K-g_R}\cdot E_\gamma/\sqrt{I^2-1}, \qquad (1.27)$$

where E_γ is the γ-transition energy.

1.5. Results of the calculations

Calculations for the isotopes ^{164,166,168,170}Er

The experimental data from Refs. 4–6 and 44–62 were used in the calculations for the isotopes ^{164,166,168,170}Er. For describing the spectrum of positive-parity states, the parameters of the model were chosen as follows.

(a) Following Ref. 63, it was assumed that at low values of the spin the energy of the rotating core coincides with the energy of the ground-state rotational band. Therefore, the inertia parameters of the rotating core $\tilde{\mathscr{I}}_0$ and $\tilde{\mathscr{I}}_1$ were determined from the condition of best agreement with the energy of the rotational states of the ground-state band up to spin $I\geqslant 8$, using (1) ($\tilde{\mathscr{I}}_0=2\alpha$, $\tilde{\mathscr{I}}_1=\frac{4}{3}\cdot\beta$).

(b) The parameters of the principal values of the energy of the gr and β bands were taken equal to the experimental values of the energy for spin $I=0$, $\omega_{gr}=E^{exp}_{gr}(0)\equiv 0$ and $\omega_\beta=E^{exp}_\beta(0)$, because they are not perturbed by the Coriolis forces. The principal energy of the $K^\pi=1^+$ band was taken to be $\omega_1\simeq 3$ MeV (Ref. 24).

(c) The free parameters of the model are η_ν, which determine the Coriolis interaction between the states of the rotational bands and the principal energy of the γ band ω_γ. They were selected to obtain the best agreement between the calculated energies of the gr, β, and γ bands and experiment.

The parameters used to calculate the energy spectrum are listed in Table I. The calculated values of the energies of the gr, β, γ, and $K^\pi=1^+$ bands are given in Ref. 14. Effects related to the Coriolis interaction can be seen in Fig. 1, where we show the dependences of the absolute values of the amplitude of the mixed states on the angular momentum for the γ-vibrational band in ^{164,166,168}Er. We see from this figure that band mixing is strongly manifested in the nuclei ^{164,168}Er, which must affect the values of the electromagnetic transition probabilities.

Next, let us consider the results of the calculations of the electromagnetic characteristics of the nuclei described above. The parameters m_0 and m_2 are determined by (1.11) and (1.12), respectively, with the experimental values of the reduced $E2$-transition probabilities from ^{164}Er (Refs. 44 and 45). They turned out to be $m_0=-7.0\pm 1.2\ e\cdot\mathrm{F}^2$ and $m_2=+30.5\pm 4.0\ e\cdot\mathrm{F}^2$.

The following expression can be written down for the ratio of the reduced probabilities of $E2$ transitions from $K^\pi=2^+$ states with odd I to the $I\pm 1$ levels of the ground-state band, using (1.10):

$$R_{I\gamma}=\frac{B(E2;I_\gamma\to(I+1)_{gr})}{B(E2;I_\gamma\to(I-1)_{gr})}$$

$$=\left|\frac{-\psi^I_{1,\gamma}+Z\psi^I_{\gamma,\gamma}\sqrt{\dfrac{I-1}{I+1}}}{\psi^I_{1,\gamma}\sqrt{\dfrac{I-1}{I+1}}+Z\psi^I_{\gamma,\gamma}}\right|^2, \qquad (1.28)$$

where $Z=m_2/m_1$.

TABLE III. Ratios of reduced $E2$-transition probabilities in ^{166}Er.

	Experiment		Theory		
$(I_\gamma \to I'_K)/(I_\gamma \to I''_{gr})$	Ref. 47	Ref. 48	Phen. Ref. 14	TRM Ref. 77	Alaga
$(2_\gamma \to 2_{gr})/(2_\gamma \to 0_{gr})$	1.86(10)	1.91	1.80	1.92	1.43
$(2_\gamma \to 4_{gr})/(2_\gamma \to 2_{gr})$	0.097(8)	0.063	0.084	0.091	0.05
$(3_\gamma \to 4_{gr})/(3_\gamma \to 2_{gr})$	0.66(5)	0.73	0.66	0.78	0.40
$(3_\gamma \to 2_\gamma)/(3_\gamma \to 2_{gr})$	-	34.3	30.8	43.8	-
$(4_\gamma \to 4_{gr})/(4_\gamma \to 2_{gr})$	5.67(45)	6.3	5.22	6.24	2.94
$(4_\gamma \to 6_{gr})/(4_\gamma \to 4_{gr})$	0.256(65)	0.186	0.191	0.21	0.086
$(4_\gamma \to 2_\gamma)/(4_\gamma \to 2_{gr})$	64.3(70)	53.5	44.7	66.8	-
$(5_\gamma \to 6_{gr})/(5_\gamma \to 4_{gr})$	1.36(10)	1.52(25)	1.2	1.66	0.57
$(5_\gamma \to 4_\gamma)/(5_\gamma \to 4_{gr})$	-	25(20)	21	33.7	-
$(6_\gamma \to 6_{gr})/(6_\gamma \to 4_{gr})$	10.9(8)	13(7)	10.0	13.6	3.7
$(6_\gamma \to 8_{gr})/(6_\gamma \to 6_{gr})$	-	0.28(16)	0.30	0.35	0.11
$(6_\gamma \to 4_\gamma)/(6_\gamma \to 4_{gr})$	241(17)	220(150)	170	283	-
$(7_\gamma \to 8_{gr})/(7_\gamma \to 6_{gr})$	2.12(18)	2.5(5)	1.73	2.96	0.67
$(7_\gamma \to 6_\gamma)/(7_\gamma \to 6_{gr})$	-	18.8(40)	14.1	26.9	-
$(8_\gamma \to 8_{gr})/(8_\gamma \to 6_{gr})$	18.9(45)	-	19.3	31.8	4.17

The parameter m_1 was determined using (1.28) from the experimental value of $R_{5\gamma}$ for $I=5$ in ^{164}Er (Ref. 17) and turned out to be $m_1 = -80.0\ e\cdot F^2$.

In Tables II–IV we give the calculated values of the ratios of the reduced probabilities for $E2$ transitions from the γ band, $R_{I\gamma}$. The calculated values R_{IK}^{theor} are compared with the various experimental values R_{IK}^{exp} and also with R_{IK}^{A} calculated using the adiabatic theory, and with R_{IK}^{theor} calculated using the two-rotor model (TRM).[77] For all the Er isotopes the ratios R_{IK} were calculated using the set of parameters m_K and $Q_0 = 742$ F^2 defined above.[4] We see from these tables that the model satisfactorily describes all the known values of R_{IK}^{exp} for these nuclei. The deviation of $R_{I\gamma}^{exp}$ from $R_{I\gamma}^{A}$ is noticeable for both even and odd spins with $I=3,5$. In the case of ^{164}Er, $R_{3\gamma}^{exp}$ differs from $R_{3\gamma}^{A}$ by a factor of two, and the difference grows with increasing I, which confirms the mixing of the γ band and the $K^\pi \neq 0^+$ band. Our model taking into account this mixing gives a satisfactory description of the deviation of R_{IK}^{exp} from the Alaga rule.

The characteristics of magnetic dipole transitions from β- and γ-vibrational bands and inside the γ band were calculated using (1.23). The parameter m'_1 was found from (1.24), using the experimental value $B(M1;00^+_{gr} \to 11^+) \simeq 1.0\ \mu_n^2$ for ^{168}Er (Ref. 24). The parameters g_K were assumed equal ($g_{K=1} = g_{K=2}$) and were found from (1.27), using the experimental value of δ for $I=4$ in ^{166}Er (Ref. 56). The calculated values of the multipole-mixture coefficient δ are given in Tables V and Tables VI and are compared with the experimental values and also with the values calculated in the two-rotor model.[77] The signs of the experimental values of δ quoted by various authors for the same transition in a given nucleus are often opposite. However, the discrepancy is only apparent: the sign of δ depends on which expressions are used to analyze the angular correlations and on the conventions followed by the authors. In this review we use the sign of δ following from the Steffen–Becker sign convention,[62] as in Ref. 4. We see from these tables that the experimental values of δ have a large spread. However, one of them agrees with δ^{theor} calculated in this model. In the tables we give the values for transitions between rotational levels of the γ and gr bands, and for transitions within the γ band.

The values of the parameter m_1 determined from the ratios of $E2$-transition probabilities turned out to be larger than in other studies. This is because in the basis states of the Hamiltonian we have included only a single band with $K^\pi = 1^+$, whereas there may be several such states, as in the nuclei ^{160,162,164}Dy and ^{172,174,176}Yb (Refs. 27 and 28). There-

TABLE IV. Ratios of reduced $E2$-transition probabilities in ^{168}Er.

	Experiment		Theory		
$(I_\gamma \to I'_{gr})/(I_\gamma \to I''_{gr})$	Ref. 49	Ref. 50	Phen. Ref. 14	TRM Ref. 77	Alaga
$(2_\gamma \to 2_{gr})/(2_\gamma \to 0_{gr})$	2.27(45)	1.79(4)	1.74	1.73	1.43
$(2_\gamma \to 4_{gr})/(2_\gamma \to 2_{gr})$	0.044(22)	0.075(4)	0.077	0.076	0.05
$(3_\gamma \to 4_{gr})/(3_\gamma \to 2_{gr})$	0.65(30)	0.64(4)	0.61	0.62	0.4
$(4_\gamma \to 4_{gr})/(4_\gamma \to 2_{gr})$	6.3(30)	5.27(55)	5.0	4.6	2.94
$(4_\gamma \to 6_{gr})/(4_\gamma \to 4_{gr})$	0.076(38)	-	0.178	0.16	0.086
$(5_\gamma \to 6_{gr})/(5_\gamma \to 4_{gr})$	1.0(4)	-	1.1	1.15	0.57
$(6_\gamma \to 6_{gr})/(6_\gamma \to 4_{gr})$	10.7(42)	-	10.6	6.9	3.7
$(6_\gamma \to 8_{gr})/(6_\gamma \to 6_{gr})$	0.19(8)	-	0.31	0.24	0.11
$(7_\gamma \to 8_{gr})/(7_\gamma \to 6_{gr})$	1.64(80)	-	1.57	1.72	0.67

TABLE V. Multipole-mixture coefficients δ for ^{164}Er.

I_i	I_f	Exp. (Ref. 51)	Phen. (Ref. 14)	TRM (Ref. 77)
2_γ	2_{gr}		−5.1	−3.6
3_γ	2_{gr}	$0.13^{+0.28}_{-0.25}$ or $-7.7^{+5.1}_{-\infty}$	−5.2	−3.1
4_γ	4_{gr}	$-1.15^{+0.35}_{-1.02}$ or >7	−2.45	−1.78
5_γ	4_{gr}	$-4.8^{+1.5}_{-5.8}$ or $0.0^{+0.07}_{-0.04}$	−3.0	−1.63
6_γ	6_{gr}	$-1.19^{+1.6}_{-1.02}$ or >3.3	−1.42	−1.16
7_γ	6_{gr}	$-6.5^{+2.2}_{-5.5}$	−2.19	−1.0
8_γ	8_{gr}	$-1.5^{+0.75}_{-3.0}$ or $12.0^{+\infty}_{-6.8}$	−0.89	−0.82

fore, the values of $B(M1)$ for transitions from 1^+ states obtained from our model may be overestimated.

The results of the calculation suggest the following conclusions, which were briefly described in Ref. 14.

1. The deviations of R_{IK} from the Alaga rule are associated with mixing of the gr, β, γ, and $K^\pi = 1^+$ bands.

2. The presence of $K^\pi = 1^+$ components in the wave functions of vibrational states leads to $M1$ transitions from these states to states of the ground-state band.

3. The values of the coefficients δ for transitions from the γ band are negative, which corresponds to most of the available experimental data. As the angular momentum increases, the coefficient δ decreases in absolute value.

4. A $K^\pi = 1^+$ state must exist in the nuclei ^{164,166}Er, and the $B(M1)$ factor from this level must be of the same order ($\approx 0.33\mu_n^2$) as in ^{168,170}Er (Ref. 24).

Calculations for the isotopes ^{156,158,160,162,164}Dy

In Figs. 2–6 we show the spectra of theoretical and experimental energies of the isotopes ^{156,158,160,162,164}Dy, respectively. Comparing them, we see that the model qualitatively reproduces the experimental values of the energies.

The structures of the states of the β and γ bands of ^{156,162}Dy obtained in the description of the energy are given in Ref. 18. In states of the γ band the β components become noticeable already at low spins. Mixing of the states of the β and γ bands is strongly manifested in ^{156,158}Dy, owing to the closeness of the principal energies.

The electric $E2$ transitions from collective states of the ground-state band were calculated using (1.10). The values of Q_0 for the calculations were taken from experiment. The parameters m_0 and m_2 were also determined from experiment,[4] using Eqs. (1.11) and (1.12) for the reduced $E2$-transition probabilities in the adiabatic approximation. The values of $B(E2)$ from the 1^+ band are not known experimentally, and so, assuming that the $B(E2)$ from states of the 1^+ band to levels of the ground-state band are identical in the adiabatic approximation (i.e., $m_1 = m_{1_1} = m_{1_2} = \ldots$), the parameter m_1 was determined from the condition of best agreement between the calculated ratios of reduced prob-

TABLE VI. Multipole-mixture coefficients δ for ^{168}Er.

I_i	I_f	Experiment		Phen. (Ref. 14)	TRM (Ref. 77)
2_γ	2_{gr}	$\lvert\delta\rvert \geq 6.4$	Ref. 57		
		$\lvert\delta\rvert \geq 29$	Ref. 52		
		or >9.4 or <−4.8	Ref. 59	−7.9	−4.4
3_γ	2_{gr}	$\lvert\delta\rvert = 8.1$	Ref. 58	−7.9	−4.0
		16.5(23)	Ref. 59		
3_γ	4_{gr}	−4.9(3)	Ref. 59	−5.5	−3.0
		$-5.7^{+5.7}_{-3.7}$	Ref. 52	−3.7	−2.5
4_γ	4_{gr}	$25^{+\infty}_{-13}$ or $50^{+\infty}_{-33}$	Ref. 57		
5_γ	4_γ	$\lvert\delta\rvert = 1.41$	Ref. 49		
		$\lvert\delta\rvert = 1.38^{+2.05}_{-0.71}$	Ref. 60	−1.6	3.3
6_γ	5_γ	$\lvert\delta\rvert = 1.05$	Ref. 49		
		$\lvert\delta\rvert = 1.55^{+1.05}_{-0.76}$	Ref. 60	−1.5	2.3
7_γ	6_γ	$\lvert\delta\rvert = 1.92$	Ref. 49		
		$\lvert\delta\rvert = 1.52^{+1.14}_{-0.82}$	Ref. 60	−1.6	3.6
8_γ	7_γ	$\lvert\delta\rvert = 0.245$	Ref. 49	−1.3	2.5

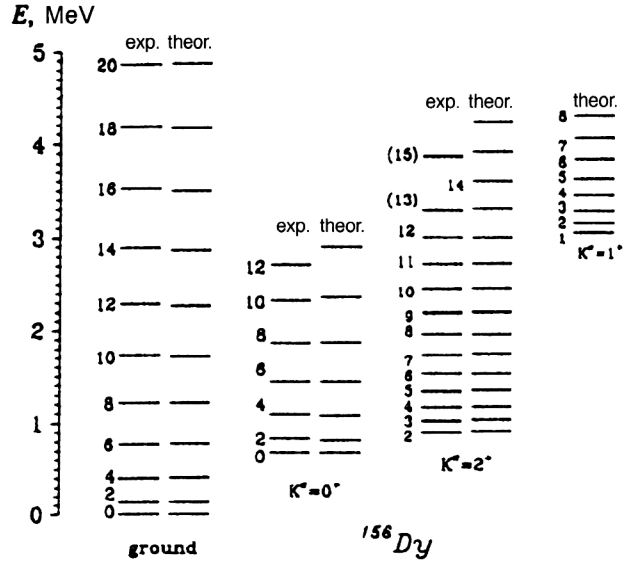

FIG. 2. Comparison of the theoretical and experimental energy spectra for ^{156}Dy.

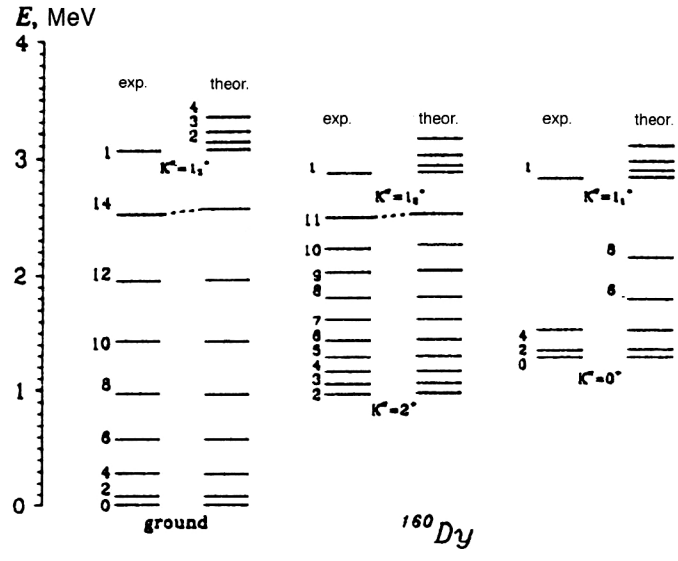

FIG. 4. Comparison of the theoretical and experimental energy spectra for ^{160}Dy.

abilities of $E2$ transitions from states of the γ band with the experimental data. In Fig. 7 we give the calculated values of $B(E2)$ for $I_\gamma \to (I-2)_{\rm gr}$, $I_\gamma \to I_{\rm gr}$, and $I_\beta \to (I-2)_{\rm gr}$ transitions and the reduced matrix elements $\langle (I+2)_{\rm gr} \| m(E2) \| I_{\rm gr} \rangle$ and $\langle I_{\rm gr} \| m(E2) \| I_{\rm gr} \rangle$ in ^{156}Dy, which are compared with experiment[19] and with the values calculated in the adiabatic approximation. We see from these figures that the nonadiabatic features of $B(E2)$ transitions from β and γ bands can be attributed to mixing of states of the gr, β, γ, and $K^\pi = 1^+$ bands.

In Tables VII and VIII we give the calculated values of the ratios of reduced probabilities of $E2$ transitions from the γ-vibrational band for the nuclei listed above. The results of the calculations agree with the experimental values $R_{I\gamma}^{\rm exp}$ (Refs. 64–70) and with those calculated using the Alaga formula. We see from the tables that the model satisfactorily describes the deviations of $R_{I\kappa}^{\rm exp}$ from the Alaga rule.

The values of the parameter m_1 characterizing $E2$ transitions from levels of the 1^+ band turned out to be larger for ^{156,158}Dy than for ^{160,162,164}Dy. This is because for the isotopes ^{156,158}Dy we included only one band with $K^\pi = 1^+$ in the basis states of the Hamiltonian, although such a level has not been found experimentally. However, several 1^+ states have been found experimentally for ^{160,162,164}Dy. The large value of m_1 in the calculations indicates that several 1^+ levels may also exist in the nuclei ^{156,158}Dy.

The $M1$ transitions from states of the β and γ bands were calculated using (1.23). The parameters m_1' were determined from (1.24), using the experimental values of $B(M1)$ from the 1_ν^+ levels.[28] The parameters g_K and g_R were found from the experimental values of the magnetic moments for the ground-state band $[\mu(4^+,{\rm gr}) = 1.48^{+0.67}_{-0.54}\,\mu_{\rm n}]$ and the γ

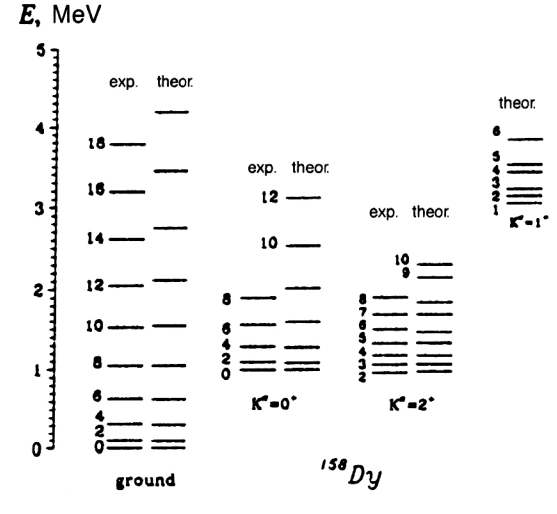

FIG. 3. Comparison of the theoretical and experimental energy spectra for ^{158}Dy.

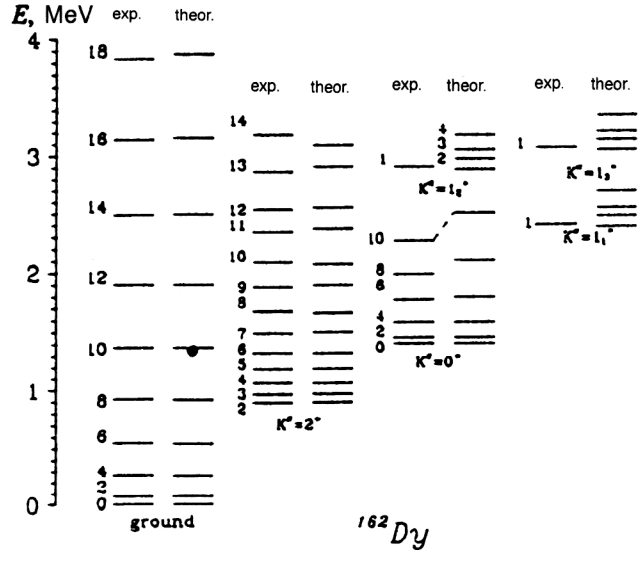

FIG. 5. Comparison of the theoretical and experimental energy spectra for ^{162}Dy.

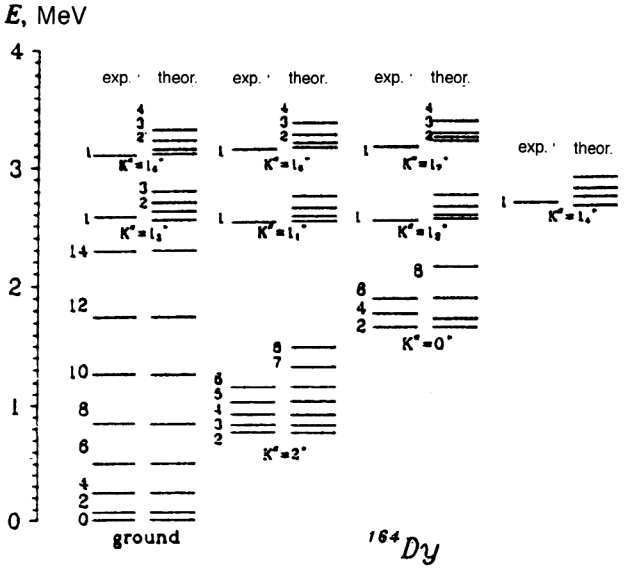

FIG. 6. Comparison of the theoretical and experimental energy spectra for ^{164}Dy.

band $[\mu(2^+,\gamma)=0.32\pm0.4\,\mu_n]$ for ^{160}Dy (Ref. 71), and turned out to be $g_K=0.10$ and $g_R=0.36$. It was shown in Ref. 72 that $g_R^{\rm exp}(4^+,{}^{158}{\rm Dy})\simeq g_R^{\rm exp}(2^+,{}^{160}{\rm Dy})\simeq g_R^{\rm exp}(2^+,{}^{162}{\rm Dy})$. Therefore, in the calculations for all the Dy isotopes we used the values of g_K and g_R found above. The calculated values of $g_R^{\rm eff}(I)=\mu(I)/I$ as a function of spin are shown in Fig. 8 for ^{158,160,162}Dy. We see from these figures that the g_R factor of the γ band at low I is smaller than in the ground-state band ($g_R^{\rm gr}$), and approaches $g_R^{\rm gr}$ with increasing I. In our scheme the values of g_R for states of the ground-state band turned out to be constant, as is confirmed by experiment for $I\leqslant 10\,\hbar$ in ^{158}Dy (Refs. 72 and 73).

Experiment[73] gives $g_R=0.04\pm0.11$ for ^{158}Dy for spins $I\simeq 14\,\hbar$ in the gr band. This is certainly related to the complex structure of the ground-state band at high spins. For example, in our scheme the mixing of the gr band with the aligned S band, which has a large moment of inertia, is not taken into account. In Fig. 9 we give the values of $B(M1)$ calculated using (1.24) for $I_\gamma\to(I\pm1)_{\rm gr}$ and $I_\gamma\to I_{\rm gr}$ transitions. In all cases $B(M1)$ increases monotonically with increasing spin, and $B(M1)$ for ^{160}Dy is always smaller than for the other nuclei.

In Table IX we compare the theoretical and experimental values of δ for ^{160,162,164}Dy. The amount of experimental data on δ for ^{160}Dy turned out to be larger than for ^{162,164}Dy, and for ^{156,158}Dy there are no data. The values of $\delta^{\rm exp}$ for transitions in the γ band are available only for ^{162}Dy, and within the experimental error they agree with the calculated values $\delta^{\rm theor}$. For $\gamma\to$gr transitions the theory is in satisfactory agreement with experiment in most cases.

The experimental values given in Ref. 69, $B(E2;2\gamma\to2{\rm gr})=0.045(25)\ e^2b^2$, $0.0446(27)\ e^2b^2$, and $0.0411\ e^2b^2$, respectively, for the isotopes ^{160,162,164}Dy, and the multipole-mixture coefficients, $\delta^{\rm exp}(2\gamma\to2{\rm gr};{}^{160}{\rm Dy})=-16.7(14)$ (Ref. 74), $\delta^{\rm exp}(2\gamma\to2{\rm gr};{}^{162}{\rm Dy})=-8.1(11)$ (Ref. 75), and $\delta^{\rm exp}(2\gamma\to2{\rm gr};{}^{164}{\rm Dy})=-5.7(12)$ (Ref. 75), allow the determination of $B^{\rm exp}(M1)$. These turned out to be $B^{\rm exp}(M1;{}^{160}{\rm Dy})=0.086(6)\times10^{-3}\mu_n^2$, $B^{\rm exp}(M1;{}^{162}{\rm Dy})=0.44(3)\times10^{-3}\mu_n^2$, and $B^{\rm exp}(M1;{}^{164}{\rm Dy})=0.42(3)\times10^{-3}\mu_n^2$. Our calculations give $B^{\rm theor}(M1;{}^{160}{\rm Dy})=0.082\times10^{-3}\mu_n^2$, $B^{\rm theor}(M1;{}^{162}{\rm Dy})=0.52\times10^{-3}\mu_n^2$, and $B^{\rm theor}(M1;{}^{164}{\rm Dy})=0.42\times10^{-3}\mu_n^2$, in good agreement with the experimental values.

Calculations for ^{156}Gd

A fairly complete analysis of states of positive and negative parity was carried out by Backlin *et al.* in Ref. 76. The ^{156}Gd nucleus is one of the best studied nuclei and one of the first nuclei in which a new type of excitation was discovered: collective $I^\pi=1^+$ states in the energy range 2–3.5 MeV (Ref. 21). At the present time, several such states have been identified in ^{156}Gd in a γ-scattering experiment.[62] In Table X we show the energies of the 1^+ collective levels, the values of the probabilities $B(M1)$, and the ratios of the reduced probabilities $R=B(M1;1^+1\to2^+{\rm gr})/B(M1;1^+1\to0^+{\rm gr})$. Three 1^+ states with energies 1966, 2027, and 2187 keV have also been observed in the β decay of ^{156}Eu (Ref. 76). Their rotational levels up to 4^+ for the first two bands and up to 3^+ for the last band have been determined. The ratios of $M1$ transitions from these levels agree with the adiabatic values calculated from the Alaga rule, and they allow the value $K^\pi=1^+$ to be assigned to these bands.[76] A level with energy 2027 keV has also been observed in a photon-scattering experiment (see Table X).

Information has been obtained from the $(\alpha,2n)$ reaction about the levels of rotational bands with $K^\pi=0_1^+$ (ground-state) up to $I=16^+$, with $K^\pi=0_2^+$ and 0_3^+ (β-vibrational) up to $I=10^+$, and with $K^\pi=2_1^+$ (γ-vibrational) up to $I=11^+$.

Calculations were performed using the model described above in order to study the properties of the levels of these bands. The gr, 0_2^+, 0_3^+, and 2_1^+ bands and all bands with $K^\pi=1^+$ known from experiment were included in the basis states of the Hamiltonian. The principal energies of the 1^+ bands were also found experimentally:

$$\omega_{1_\nu}=E_{1_\nu}^{\rm exp}(I=1)-E_{\rm core}^{\rm theor}(I=1).$$

In Fig. 10 we give the theoretical and experimental energies of the positive-parity states.

The structure of states of the gr, 0_2^+, 0_3^+, and 2_1^+ bands is given in Ref. 20. The ground-state band is more pure than the 0_2^+, 0_3^+, and 2_1^+ bands, where mixing can be strongly manifested. The states of the 0_3^+ and 2_1^+ bands are especially strongly mixed. This leads to nonadiabatic features in the probabilities for electromagnetic transitions between states of positive-parity bands, in particular, for $E0$ transitions from states of the 2_1^+ band to rotational levels of the ground-state band.

We shall calculate the reduced $E2$-transition probabilities using (1.10). In the calculations the value of the internal quadrupole moment was taken to be $Q_0=6.81(6)$ b (Ref. 4). The values of m_K were chosen for the transitions from each band in order to obtain the best agreement between the $E2$-transition probabilities and the experimental data. In Tables XI and XII we show the ratios of $E2$-transition prob-

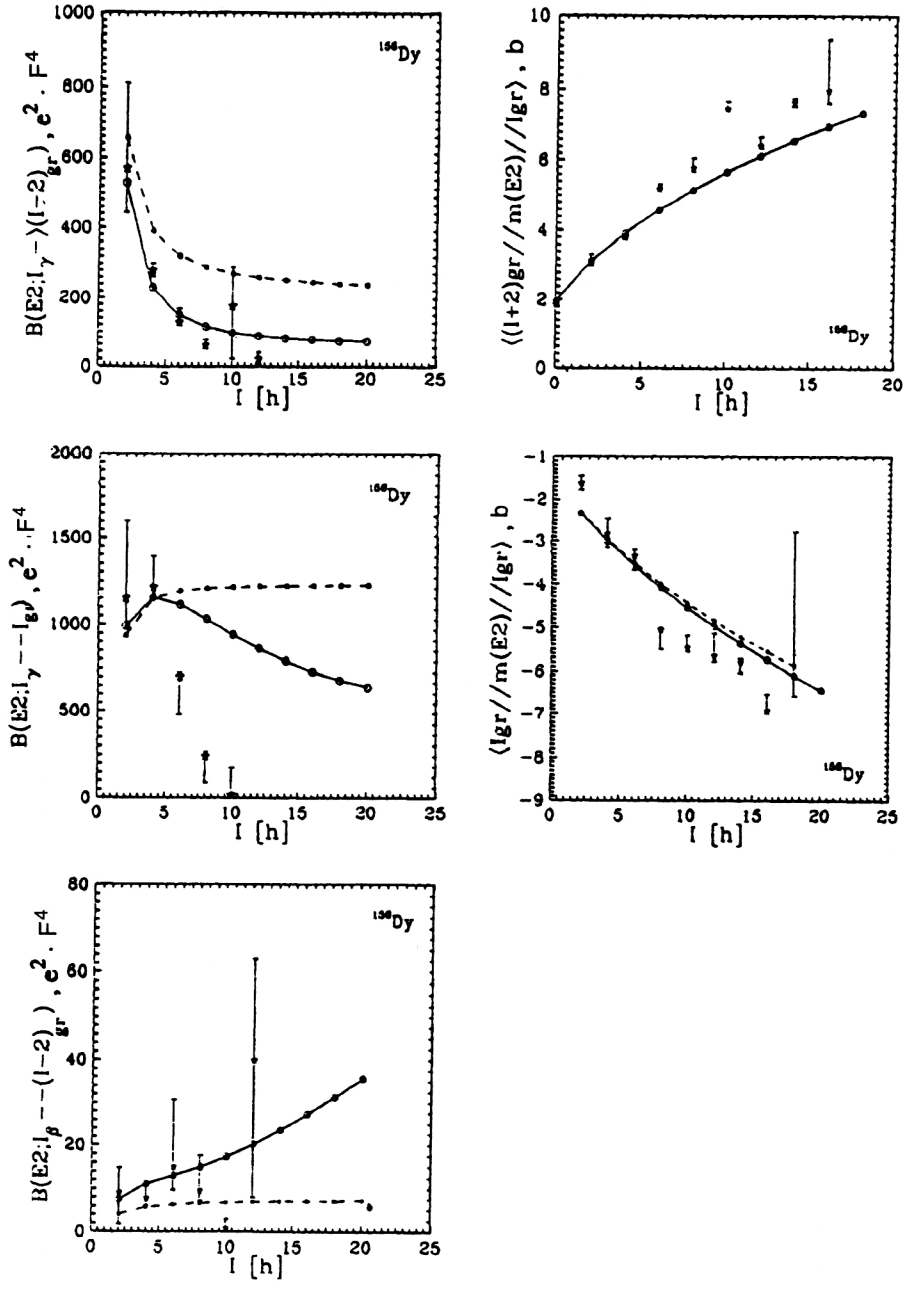

FIG. 7. Reduced probabilities and matrix elements of $E2$ transitions for ^{156}Dy (*—experiment,[19] ○—theory, and ●—the adiabatic values).

abilities from the 0_2^+ and 2_1^+ bands, respectively. The largest deviations from the Alaga rule are observed for the ratios R_{IK} from states of the $\beta(0_2^+)$ band. This is because β states are less strongly collectivized than $\gamma(2_1^+)$ states, and the small component of β band in the wave functions leads to significant deviations from the adiabatic theory. We see from

TABLE VII. Ratios of reduced $E2$-transition probabilities $B(E2;I_\gamma \to I_1\text{gr})/B(E2;I_\gamma \to I_2\text{gr})$ (Ref. 18).

			^{156}Dy		^{158}Dy		
I	I_1	I_2	Exp. (Ref. 64)	Theor.	Exp. (Ref. 65)	Theor.	Alaga
2	0	2	0.60(9)	0.53	0.44(9)	0.55	0.7
3	2	4	0.37(6)	1.2	1.72(35)	1.20	2.5
4	2	4	0.15(2)	0.21	0.21(4)	0.22	0.34
5	4	6	0.21(2)	0.62	0.77(15)	0.58	1.57
6	4	6	0.20(3)	0.17	0.26(10)	0.12	0.27
8	6	8	0.18(2)	0.18	-	0.03	0.24
9	8	10	0.07(2)	0.31	-	0.24	1.38

TABLE VIII. Ratios of reduced $E2$-transition probabilities $B(E2;I_\gamma \to I_1\text{gr})/B(E2;I_\gamma \to I_2\text{gr})$ (Ref. 18).

			^{160}Dy		^{162}Dy		^{164}Dy		
I	I_1	I_2	Exp. (Ref. 66)	Theor.	Exp. (Refs. 67 and 68)	Theor.	Exp. (Refs. 69 and 70)	Theor.	Alaga
2	0	2	0.58(6)	0.59	0.56(2)	0.58	0.55(3)	0.55	0.7
3	2	4	1.5(2)	1.64	1.61(7)	1.58	1.35(15)	1.33	2.5
4	2	4	0.22(4)	0.23	0.20(1)	0.21	0.30(4)	0.19	0.34
5	4	6	0.83(14)	0.93	0.92(6)	0.87	0.5	0.69	1.75
6	4	6	0.17(5)	0.15	0.16(3)	0.13	0.22(2)	0.10	0.27
2	4	2	0.06(1)	0.08	0.07(1)	0.08	0.11(1)	0.08	0.05

these tables that the model satisfactorily reproduces the experimental data.

In Table XIII we compare the experimental and adiabatic values of the reduced probability of $E2$ transitions to the ground-state band together with the values calculated using the interacting-boson approximation[78] (IBA) and our model. We see from this table that the adiabatic values of $B(E2)$ are in good agreement with the experimental data, and so it can be concluded that at these spins the ground-state band hardly mixes at all with the other bands. This is

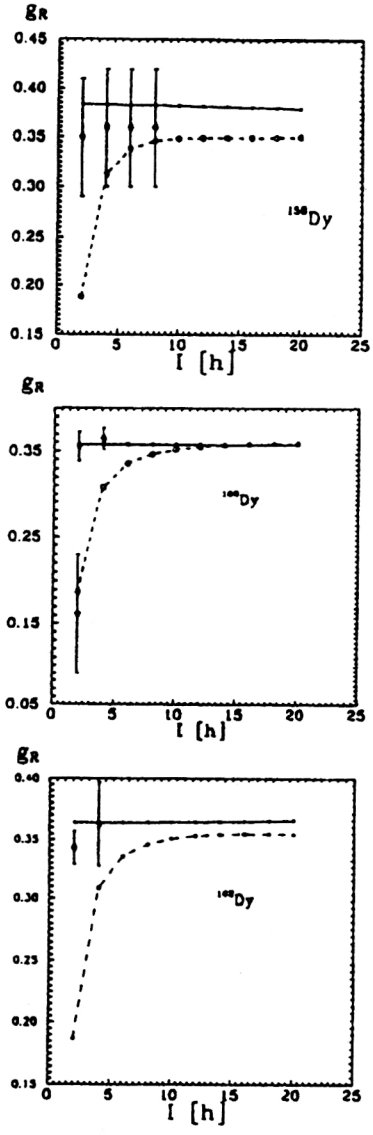

FIG. 8. Spin dependence of the g_R factor for ^{158,160,162}Dy (◇—experiment for states of the ground-state band; ▽—experiment for the γ band; ○—theory for the γ band; ●—theoretical values for the ground-state band.

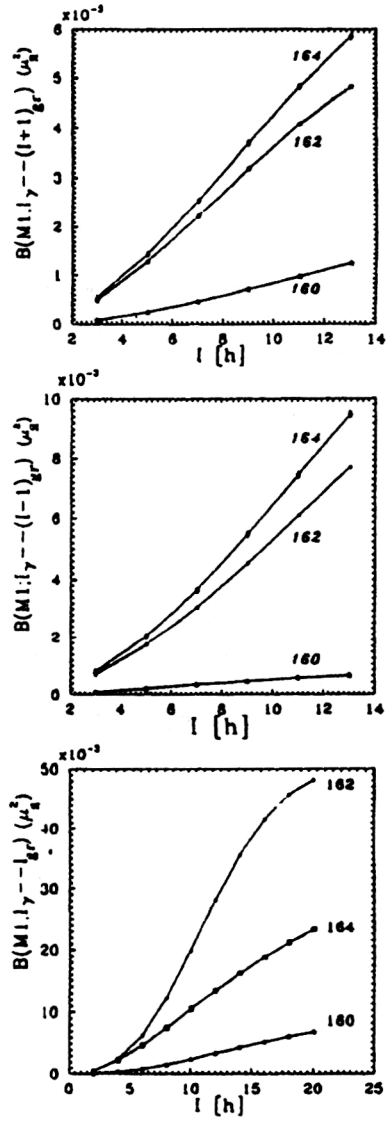

FIG. 9. Theoretical values of $B(M1)$ (*—for ^{160}Dy; ●—for ^{162}Dy; ◇—for ^{164}Dy).

TABLE IX. Values of the coefficients δ for Dy isotopes (Ref. 19).

		^{160}Dy		^{162}Dy		^{164}Dy	
I_i	I_f	Exp. (Ref. 99)	Theor.	Exp. (Ref. 68)	Theor.	Exp. (Ref. 68)	Theor.
2_γ	2_{gr}	$\delta>0.5$	14.1	$-8.3<\delta<3.4$	−5.64	$-16.3<\delta<31.5$	−5.22
4_γ	4_{gr}	$<1;>-8$	7.62	$-5.3^{+4.7}_{-0.8}$	−2.65	$-0.87^{+0.11}_{-0.13}$	−2.63
6_γ	6_{gr}	$\delta>1.4$	4.96	$-17.9<\delta<2.3$	−1.64	-	−1.78
8_γ	8_{gr}	$\delta>1.5$	3.5	-	−1.08	-	−1.80
10_γ	10_{gr}	$<-2.7;>1.2$	2.6	-	−0.74	-	−1.39
3_γ	2_{gr}	$\delta>11.0$	15.8	$-2.6^{+1.6}_{-5.3}$	−5.27	$-6.7<\delta<55.5$	−4.48
5_γ	4_{gr}	$<8;>-14.0$	10.3	$\delta<62.7$	−2.72	$-5.5^{+2.1}_{-6.1}$	−2.54
7_γ	6_{gr}	7.2(10)	6.9	-	−2.13	-	−1.76
9_γ	8_{gr}	7.0(12)	5.8	-	−1.65	-	−1.31
11_γ	10_{gr}	$\delta>0.0$	5.0	-	−1.33	-	−1.13
3_γ	4_{gr}	−0.05(5)	9.7	$-11.7<\delta<10.4$	−5.41	$-5.4^{+3.2}_{-2.5}$	−3.63
5_γ	6_{gr}	$\delta>10$	6.1	$-3.9^{+1.5}_{-4.1}$	−2.60	-	−2.31
7_γ	8_{gr}	5(8)	4.7	-	−1.95	-	−1.72
4_γ	3_γ	-	−0.77	$\lvert\delta\rvert=1.2(80)$	−0.67	-	−0.60
5_γ	4_γ	-	−0.75	$\lvert\delta\rvert=1.2(8)$	−0.66	-	−0.59
6_γ	5_γ	-	−0.70	$\lvert\delta\rvert=0.67$	−0.63	-	−0.59

confirmed by the results of the calculations performed using our model.

Using the experimental values $X_0(E0/E2)=0.23(1)$ and 0.031(13) (Ref. 4) for transitions from the 0_2 and 0_3 levels, respectively, from Eq. (1.17) we find the numerical values of the matrix elements $m'_{0_2}=0.058(1)$ eb and $m'_{0_3}=0.023(4)$ eb. We used the following values of the parameters m_{0_ν}: $m_{0_2}=0.12$ eb and $m_{0_3}=0.13$ eb. Then we used Eq. (1.15) to calculate the reduced probability $B(E0)$. In Table XIV we give the numerical values of $X_1(E0/E2)$, which are compared with the experimental values[4,41,83] and with the values calculated using the adiabatic expression (1.16). In Table XIV we also give the values of $B^{\text{theor}}(E2)$ calculated using (1.10), and the adiabatic values of $B(E2)$ found from the expression

$$B(E2;I0_\nu\to I\text{gr})=m^2_{0_\nu}\frac{I(I+1)}{(2I-1)(2I+3)}. \tag{1.29}$$

We see from this table that as the angular momentum increases, the difference between the experimental values of $X_I(E0/E2)$ and the values calculated using the Alaga rule increases. That is, with increasing I the adiabatic values of $X_I(E0/E2)$ for transitions from 0^+_2 and 0^+_3 bands increase slowly, and for some I approach the limiting value, while the experimental values of $X_I(E0/E2)$ tend to decrease. This is explained as follows:

(a) In the adiabatic approximation $B(E0)$ is a constant, and so the parameter $X^{\text{A}}_I(E0/E2)$ increases, owing to the behavior of $B^{\text{A}}(E2)$ (see Table XIV).

(b) The mixing of positive-parity states causes $B(E0)$ to decrease with spin I and $B(E2)$ to increase, which leads to decrease of $X_I(E0/E2)$.

Let us calculate the dimensionless nuclear parameter of the $E0$ transition, which depends on the structure of nuclear matter:

$$\rho(E0;I0^+_\nu\to I\text{gr})=\frac{\langle I\text{gr}\|m(E0)\|I0^+_\nu\rangle}{eR^2_0}, \tag{1.30}$$

where $R_0=r_0A^{1/3}$ and $r_0=1.2$ F.

In Fig. 11 we compare the calculated and experimental values of $\rho(E0)$. We see from this figure that for transitions from the 0^+_2 band the theoretical values of $\rho(E0)$ agree with experiment within the error, while there is qualitative agreement for transitions from the 0_3 band.

The experimental values of $\rho(E0)$ were determined using Eq. (1.30). Here we have used the data for $X_I(E0/E2)$ and $B(E2)$ given in Table XIV.

In the ^{156}Gd nucleus, $E0$ transitions from the 2^+, 1828 keV and 3^+, 1916 keV states of the $K^\pi=2^+_2$ band to the $K^\pi=2^+_1$ levels are observed, with the large values $X_2(E0/E2)=1.2$ and $X_3(E0/E2)=1.0$. This is probably related to the fact that there are few $E2$ transitions between one-phonon states, because such transitions occur mainly owing to the gr components in states of the 2^+_1 and 2^+_2 bands.

Our calculations including the Coriolis mixing of positive-parity states reproduce the experimental data well. Our model qualitatively describes the experimental values of the energy spectrum and the probabilities of electric quadrupole transitions from states of the 0^+_2, 0^+_3, and 2^+_1 bands to

TABLE X. Characteristics of 1^+ states (Ref. 79).

E_1 keV	R_{exp}	$B(M1)\uparrow$ (μ^2_n)
2027	0.25(24)	0.16(5)
2974	0.45(8)	0.35(7)
3010	0.53(23)	0.09(2)
3050	0.39(17)	0.11(3)
3070	0.64(7)	1.21(23)
3122	0.47(20)	0.09(3)
3158	0.50(13)	0.34(7)
3218	0.48(11)	0.31(6)

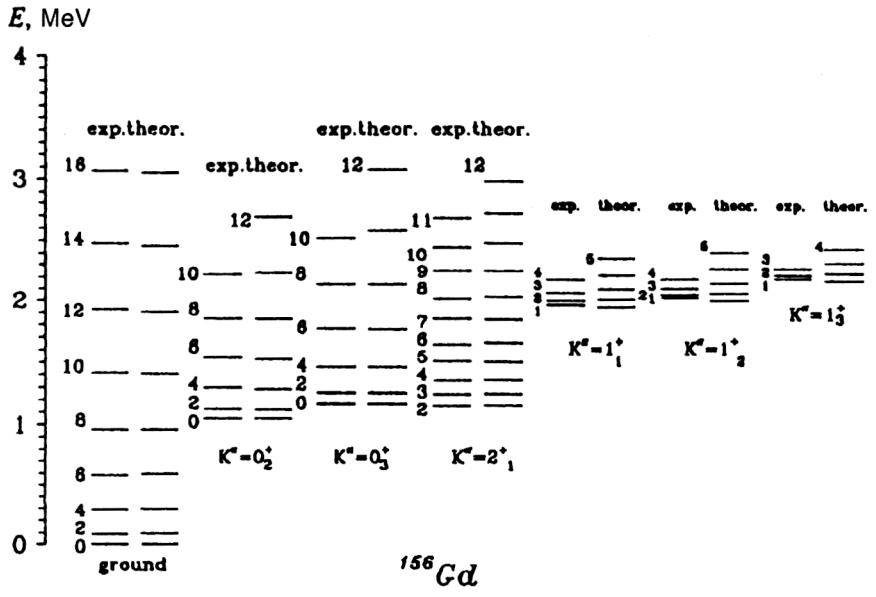

FIG. 10. Energies of positive-parity states in ^{156}Gd.

the rotational levels of the ground-state band. Therefore, our theoretical analysis seems capable of explaining the deviations from the Alaga rule of the ratios of reduced $E2$-transition probabilities $R_{IK}=B(E2;IK\to I_1\mathrm{gr})/B(E2;IK\to I_2\mathrm{gr})$, the mixing parameter of $E0$ and $E2$ transitions $X_1(E0/E2)$, and the matrix element of the $E0$ transition $\rho(E0)$.

Our analysis leads to the following preliminary conclusions:

(a) The deviations from the Alaga rule of the ratio of reduced probabilities R_{IK} for $E2$ transitions from states of the β- and γ-vibrational bands can be attributed to mixing of the ground-state, β, γ, and $K^\pi=1^+_\nu$ bands. The largest deviations from the adiabatic theory for the ratios R_{IK} from states of the $\beta(0_2^+)$ band are due to the fact that the β states are less strongly collectivized than the $\gamma(2_1^+)$ states, and a small component of the β band in the wave functions leads to significant deviations from the Alaga rule.

(b) The mixing coefficients $\delta(E2/M1)$ for transitions from states of the γ band are negative for the isotopes ^{164,166,168,170}Er and ^{162,164}Dy and positive for ^{160}Dy, in agreement with most of the available experimental data. The absolute value of the coefficient δ decreases with increasing angular momentum.

(c) In the adiabatic approximation $B(E0)$ is a constant, i.e., it does not change as the rate of rotation of the nucleus increases. The mixing of positive-parity states causes $B(E0)$ to decrease with spin I and $B(E2)$ to increase, which causes the Rasmussen parameter $X_I(E0/E2)$ to decrease (an example is the ^{156}Gd nucleus).

The results described in this section show that it is necessary to include the Coriolis interaction of states of low-lying bands with 1^+ levels. In the calculations for the isotopes ^{164,166}Er and ^{156,158}Dy, in which there is only one $K^\pi=1^+$ state, the empirical values of the parameter $\langle 2^+_\gamma|j_x|1^+\rangle$ describing the Coriolis interaction between states of the 1^+ and γ bands turned out to be larger than the values at the spherical limit (see Table I and Ref. 18). In these nuclei a similar picture is also observed for the matrix elements $\langle 0_{gr}|E2|1^+\rangle$ (see Ref. 18). However, a large number of $I^\pi=1^+$ states can be located in the excitation energy range 2–5 MeV, and the set of these states is described phe-

TABLE XI. Ratios of reduced $E2$-transition probabilities $R_I=B(E2;I0_2\to I_1\mathrm{gr})/B(E2;I0_2\to I_2\mathrm{gr})$ (Ref. 20).

I	I_1	I_2	R_I		
			Exp.	Theor.	Alaga
2	2	0	5.1 (5)^B		
			2.7 (7)*	4.1	1.43
			3.45 (34)^D		
2	4	2	1.1 (1)^B	0.74	1.80
			0.84 (8)^A		
4	4	2	2.3 (2)^B	2.4	0.91
4	6	4	0.65 (9)^B	0.32	1.75
			0.7 (3)*		
6	6	4	1.2 (8)*	1.8	0.81
10	10	8	>1.7*	1.33	0.74

*—from Ref. 78; A—from Ref. 69; B—from Ref. 76; D—from Ref. 80.

TABLE XII. Ratios of reduced $E2$-transition probabilities $R_I = B(E2;I2_1 \to I_1\text{gr})/B(E2;I2_1 \to I_2\text{gr})$ (Ref. 20).

			R_I		
I	I_1	I_2	Exp.	Theor.	Alaga
2	2	0	1.75 (55)[A]		
			1.60 (9)[B]		
			1.56 (17)[C]	1.90	1.43
			1.96 (22)[D]		
			1.60 (12)[E]		
2	4	2	0.090 (9)[B]		
			0.105 (3)[C]	0.060	0.05
			0.14 (2)[E]		
3	4	2	0.56 (21)[A]		
			0.695 (8)[C]	0.65	0.40
			0.77 (15)[E]		
4	4	2	5.81 (24)[C]	4.4	2.94
			5.9 (6)[E]		
5	6	4	1.22 (16)[A]		
			1.45 (19)[C]	1.16	0.57
			1.40 (16)[E]		
6	6	4	5.9 (14)[A]	5.55	3.7
7	8	6	2.0 (12)[A]	1.62	0.67
9	10	8	2.5 (12)[A]	2.1	0.72
10	10	8	$\simeq 5$[A]	6.6	4.48

A—from Ref. 78; *B*—from Ref. 69; *C*—from Ref. 81; *D*—from Ref. 80; *E*—from Ref. 76.

nomenologically as a collective state of the scissors mode. It would certainly be interesting to obtain a description of the mixing of states using a microscopic model including all 1^+ states and with matrix elements of the Coriolis interaction that are not free parameters. This problem has been discussed in Refs. 84 and 85, where a microscopic analysis was carried out using the RPA with accurate isolation of ghost admixtures due to violation of the rotational invariance of the Hamiltonian.

In Fig. 12 we show the correlation between collective 1^+_ν states and the Coriolis matrix elements.[84] We see from this figure that the more strongly collectivized 1^+_ν states have large matrix elements connecting them to the γ band.

It should be noted that the reduced $E2$ matrix elements $\langle 0^+_{\text{gr}}|E2|1^+_\nu\rangle$ are mainly positive, while the matrix elements of the Coriolis interaction $\langle 2^+_\gamma|j^+|1^+_\nu\rangle$ are negative (see Fig. 12). This implies that the contribution of 1^+_ν states to the matrix elements of $E2$ transitions are coherent. This enhances the nonadiabaticity of $E2$ transitions due to the interaction with 1^+_ν states.

It was also shown in Ref. 84 that if the rotational invariance is preserved correctly in the RPA calculations, the Coriolis interaction between the ground-state and 1^+ bands must be exactly zero, and 1^+_ν bands are coupled by Coriolis forces only to the γ band. However, the experimental data suggest the presence of coupling between the ground-state band and other bands. To exclude the coupling between the ground-state band and the 1^+ and γ bands, it is necessary to generalize the approximation, for example, by taking into account the γ deformation or the relative motion of the proton and neutron components, which is considered in the following section. It will be shown that the internal angular-momentum operator is not the only operator describing the

TABLE XIII. Experimental and theoretical values of the reduced $E2$-transition probability in the ground-state band (Ref. 20).

	$B(E2;I^+\text{gr}\to(I-2)^+\text{gr})\times 10^4\ e^2\ \text{F}^4$			
I	Exp. (Ref. 82)	IBA (Ref. 78)	Theor.	Adiab.
2	0.92 (3)	0.92	0.91	0.92
4	1.29 (2)	1.29	1.29	1.31
6	1.47 (4)	1.39	1.43	1.44
8	1.57 (15)	1.39	1.50	1.51
10	1.59 (9)	1.34	1.55	1.55

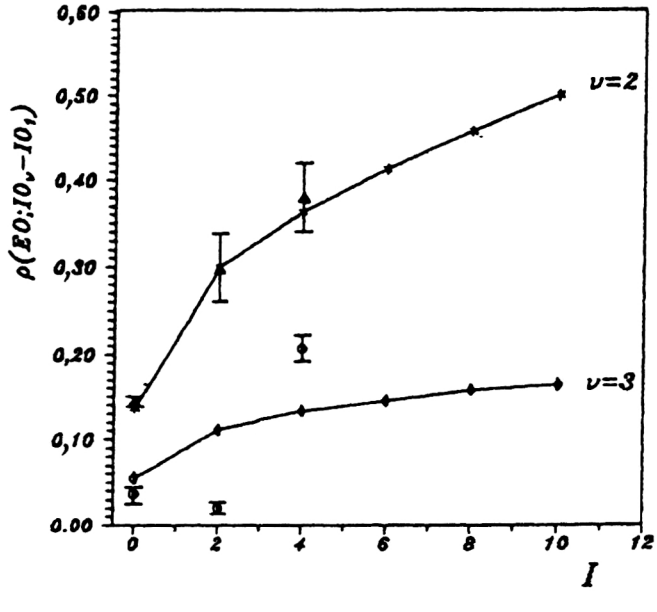

FIG. 11. Dependence of the dimensionless matrix element $\rho(E0;I0_\nu \to I\text{gr})$ on the spin I.

TABLE XIV. Characteristics of $E0$ transitions between excited states of ^{156}Gd (Ref. 20).

$I^\pi K_\nu$	E_{level} keV	E_γ keV	$X_I(E0/E2)$ Exp.	$X_I(E0/E2)$ Theor.	$X_I(E0/E2)$ Adiab.	$B(E2)\times10^{-4}$ e^2b^2 Theor.	$B(E2)\times10^{-4}$ e^2b^2 Adiab.
0^+0_2	1049	1049	0.23 (1)^A	0.23	0.23	144	144
2^+0_2	1258	1168	0.19 (5)^B	0.240	0.762	130	41
4^+0_2	1298	1010	0.20 (4)^B	0.091	0.838	277	37
6^+0_2	1540	956	0.18 (8)^B	0.071	0.855	318	37
8^+0_2	1848	883	0.05–0.08^B	0.065	0.862	331	36
10^+0_2	2220	804	0.06 (3)^B	0.061	0.865	335	36
0^+0_3	1168	1168	0.031 (13)^A	0.031	0.031	169	169
2^+0_3	1258	1169	0.017 (9)^C	0.096	0.105	45	48
4^+0_3	1462	1174	0.036 (4)^C	0.057	0.115	60	44
6^+0_3	1766	1181	-	0.040	0.117	71	43
8^+0_3	2134	1169	-	0.033	0.118	77	43
10^+0_3	2523	1107	-	0.028	0.119	81	43

A—from Ref. 4; *B*—from Ref. 41; *C*—from Ref. 83.

coupling with the dependence on the quantum numbers I and K characteristic of Coriolis mixing.

2. THE GIANT ANGULAR RESONANCE AND STRUCTURE OF THE LOWEST-LYING NUCLEAR STATES

In Sec. 1 we remarked that it is possible to describe the nonadiabatic characteristics of states of low-lying bands of deformed nuclei using models which include the Coriolis mixing of the levels of these bands with a band having the quantum characteristics $K^\pi = 1^+$. The calculation performed using the RPA,[84,85] which contains an analysis of nonadiabatic effects from the viewpoint of the microscopic approach, to some degree justifies this phenomenological treatment, as it indicates that there is coherence between the matrix elements of the Coriolis interaction and the electric quadrupole moment between states of the γ-vibrational band and the numerous 1^+ states in the vicinity of the "scissors" excitation mode. At the same time, the microscopic treatment poses the question of the nature of the coupling between the ground and 1^+ states, traces of which are present in the experimental data and are taken into account in the phenomenological approach on an equal footing with the coupling of the 1^+ and other excited bands.

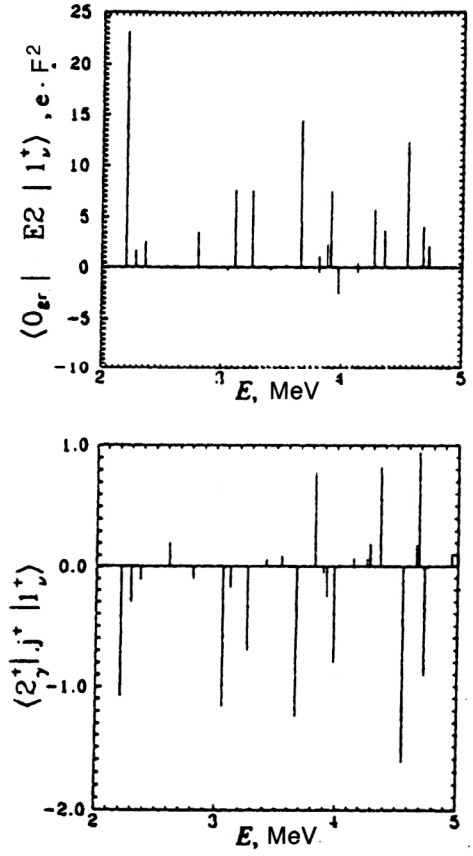

FIG. 12. Calculated values of the $E2$ matrix elements $\langle 0^+_{gr}|E2|1^+_\nu\rangle$ and the matrix elements of the Coriolis interaction $\langle 2^+_\gamma|j^+|1^+_\nu\rangle$ for ^{166}Er (Ref. 84).

In this section we discuss the physical reasons for this mixing. We assume that states of the $K^\pi = 1^+$ band correspond to excitation of the giant angular resonance predicted theoretically in Refs. 39 and 40 and induced by the relative deviation of the symmetry axes of the proton and neutron components of the nucleus. These excitations have been studied in detail theoretically using various approaches and have been identified experimentally in some nuclei.[21–28] It has proved possible to use this assumption as the basis for a model containing a small number of parameters which describes nonadiabatic effects in the spectrum of rotational bands and in the electromagnetic characteristics of positive-parity states of deformed even–even nuclei.

2.1. The two-rotor model of the nucleus

Following Ref. 40, we shall consider a model of the nucleus described as two axial rotors (proton and neutron) which can rotate relative to each other as shown in Fig. 13. We introduce the variable θ, equal to half the angle between the symmetry axes of the rotors, the direction of which is determined by the unit vectors ζ_p and ζ_n:

$$\cos(2\theta) = \zeta_p \cdot \zeta_n, \quad 0 \leqslant \theta \leqslant \pi/2. \tag{2.1}$$

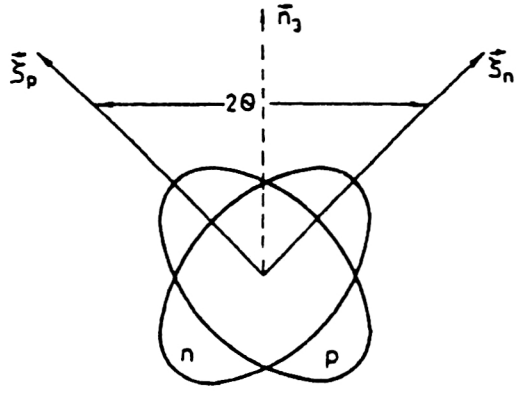

FIG. 13. Relative motion of the neutron and proton rotors.

We define the orientation of the nucleus as a whole by a right-handed orthonormal triplet of vectors:

$$\mathbf{n}_1=[\boldsymbol{\zeta}_p\boldsymbol{\zeta}_n]/\sin(2\theta),\quad \mathbf{n}_2=(\boldsymbol{\zeta}_p-\boldsymbol{\zeta}_n)/2\sin\theta,$$
$$\mathbf{n}_3=(\boldsymbol{\zeta}_p+\boldsymbol{\zeta}_n)/2\cos\theta. \tag{2.2}$$

The motion in the direction of the angle θ is counteracted by a force whose contribution to the energy is given by the function $V(\theta)$. For $\theta\leqslant\pi/4$ (or for $\pi/2-\theta\ll\pi/4$) we assume that

$$V(\theta)=c\,\theta^2/2\quad (V(\pi/2-\theta)=c(\pi/2-\theta)/2). \tag{2.3}$$

In Ref. 40 the proton and neutron components are treated as structureless systems. Here we allow these subsystems to have internal excitations with properties typical of axial nuclei. More specifically, the internal states of each subsystem are characterized by the conserved quantum number corresponding to the projection of the internal angular momentum on the symmetry axis of the subsystem (k_p, k_n). These numbers coincide with the projection of the total proton (neutron) angular momentum on the symmetry axis of the proton (neutron) component of the nucleus:

$$(\boldsymbol{\zeta}_p\mathbf{I}_p)\Psi=k_p\Psi,\quad (\boldsymbol{\zeta}_n\mathbf{I}_n)\Psi=k_n\Psi. \tag{2.4}$$

According to Refs. 86 and 87, the nuclear Hamiltonian is written as

$$\mathbf{H}=\mathbf{H}_{0,0}+\mathbf{H}_{0,1}+\mathbf{T}'_\beta+\mathbf{T}'_\gamma, \tag{2.5}$$

where

$$\mathbf{H}_{0,0}=\tfrac{1}{4}(A_p^0+A_n^0)(\mathbf{I}^2+\mathbf{S}^2)+V(\theta)+\mathbf{H}_{\rm int}, \tag{2.6}$$
$$\mathbf{H}_{0,1}=\tfrac{1}{2}(A_p^0-A^0)(\mathbf{IS}), \tag{2.7}$$
$$\mathbf{T}'=\mathbf{T}'_\beta+\mathbf{T}'_\gamma, \tag{2.8}$$
$$\mathbf{T}'_\beta=a_{\beta,1}(\mathbf{H}_{0,0}-V(\theta)-\mathbf{H}_{\rm int})+a_{\beta,2}\mathbf{H}_{0,1},$$
$$\mathbf{T}'_\gamma=\mathbf{T}'_1+\mathbf{T}'_2+\mathbf{T}'_3=b_1\mathbf{I}_+^2+\mathbf{I}_-^2b_1^+ +b_2(\mathbf{I}_+\mathbf{S}_+ +\mathbf{S}_+\mathbf{I}_+)$$
$$+(\mathbf{S}_-\mathbf{I}_- +\mathbf{I}_-\mathbf{S}_-)b_2^+ +b_1\mathbf{S}_+^2+\mathbf{S}_-^2b_1. \tag{2.9}$$

Here A_i^0 are numerical parameters ($A_i^0=1/(2\mathscr{T}_i)$, where $\mathscr{T}_i$ is the moment of inertia of the ith subsystem), $\mathbf{I}=\mathbf{I}_p+\mathbf{I}_n$ is the total angular momentum, and $\mathbf{S}=\mathbf{I}_p-\mathbf{I}_n$ is the operator for the relative motion of the two rotors.

The eigenfunctions of $\mathbf{H}_{0,0}$ describing the system with axial symmetry are sought in the form[86,87]

$$\Psi(IMkK\kappa n)=\left(\frac{2I+1}{16\pi^2}\right)^{1/2}(1+\delta_{K,0}\delta_{k,0})^{-1/2}\varphi_{\kappa,n}(x)$$
$$\times(D^I_{MK}(\alpha,\beta,\gamma)\chi_k+(-1)^{I+K}$$
$$\times D^I_{M,-K}(\alpha,\beta,\gamma)\chi_{-k}). \tag{2.10}$$

Here

$$K\geqslant 0,\quad k=k_p+k_n,\quad \kappa=|k-K|=0,1,2,\ldots,$$
$$n=0,1,2,\ldots. \tag{2.11}$$

For the function $\varphi_{\kappa,n}(x)$ we find the equation

$$\frac{\omega}{2}\left(-\frac{\partial}{\partial x^2}+\frac{1}{x^2}\left(\kappa^2-\frac{1}{4}\right)+x^2\right)\varphi_{\kappa,n}(x)=\mathscr{E}_{\kappa,n}\varphi_{\kappa,n}(x), \tag{2.12}$$

which is the same as the equation considered in Ref. 40. The following expressions are obtained[40] for the eigenvalue spectrum $\mathscr{E}_{\kappa,n}$ and the eigenfunctions:

$$\mathscr{E}_{\kappa,n}=\omega(2n+\kappa+1), \tag{2.13}$$

$$\varphi_{\kappa,n}(x)=\left(\frac{2n!}{(n+\kappa)!}\right)^{1/2}x^{\kappa+1/2}e^{-x^2/2}L_n^\kappa(x^2), \tag{2.14}$$

where $L_n^\kappa(x^2)$ is the associated Laguerre polynomial.

The energy spectrum of the operator $\tilde{\mathbf{H}}_{0,0}$ is therefore given by

$$E(IkK\kappa n)=\frac{1}{2}\omega\theta_0^2I(I+1)+\omega(2n+\kappa+1)+\mathscr{E}_{\rm int}(k). \tag{2.15}$$

The spectrum is shown schematically in Fig. 14. The projections of the angular momentum of the internal motion on the nuclear axis (k) and the precessional motion of the neutron and proton components (κ) can point in the same direction ($k>0$) or opposite to each other ($k<0$). Therefore, excitation of the relative motion of the protons and neutrons for an internal configuration with angular-momentum projection k on the approximate symmetry axis can either increase or decrease the number K.

The motion of the neutrons relative to the protons may be accompanied by excitation of β or γ states. As a result, above the ground and β- and γ-vibrational states there is an infinite series of levels with quantum characteristics $(k=0,K=\kappa=1,n)_{\rm gr}$, $(k=0,K=\kappa=1,n)_\beta$, and $(k=2,K=1,3;\ \kappa=1,n)_\gamma$, respectively. These states are connected to the ground and β- and γ-vibrational states by dipole magnetic transitions. The states $(k=0,K=\kappa=1,n=0)_\beta$ and $(k=2,K=1,3;\ \kappa=1,n=0)_\gamma$ have not yet been seen experimentally. However, in Ref. 31 calculations were performed using the quasiparticle–phonon model for the isotopes ^{156,158}Gd, and it was shown that some 1^+ states have stronger $M1$ transitions to excited states of the nucleus rather than to the ground state.

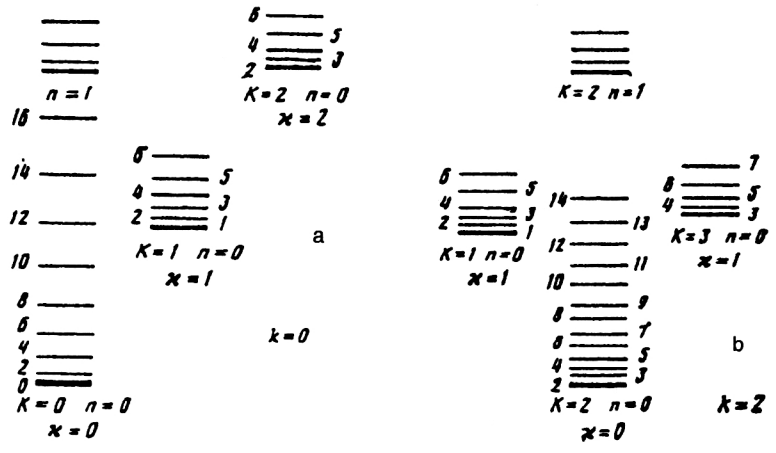

FIG. 14. Level scheme.

The operator $\mathbf{H}_{0,1}$ is nondiagonal in the basis functions (2.10) and (2.14) and leads to the mixing of states with different n, κ, and K in its eigenfunctions. The nonzero matrix elements of $\mathbf{H}_{0,1}$ are

$$\begin{aligned}\langle IMk,K\pm1,\kappa+1,n'|\mathbf{H}_{0,1}|IMkK\kappa n\rangle&=\tfrac{1}{2}\omega\theta_0\frac{A_p^0-A_n^0}{A_p^0+A_n^0}((I\mp K)(I\pm K-1)\\&\times[1+(-1)^I\delta_{K,0}\delta_{k,0}])^{1/2}\\&\times\left\{-\frac{n\pm K+1}{(n+\kappa+1)^{1/2}}\delta_{n,n'}+(\kappa\mp K)\right.\\&\times\left.\left(\frac{(n)!(n+\kappa)!}{n!(n'+\kappa+1)!}\right)^{1/2}-\sqrt{n}\delta_{n',n-1}\right\}\quad(n'>n).\end{aligned}\tag{2.16}$$

This matrix element describes a coupling between the states with the dependence on the quantum numbers I and K characteristic of Coriolis mixing. However, the operator $\mathbf{H}_{0,1}$ in the matrix element involves not the sum of internal angular momenta of the proton and neutron components $\mathbf{J}_+=\mathbf{J}_p^+ + \mathbf{J}_n^+$, but their difference $\mathbf{S}$ [see Eq. (2.7)].

2.2. The mixing of states with different internal structure

Let us now consider the properties of the operator $\mathbf{T}'$ in Eq. (2.8). We shall deal with each of the terms in Eqs. (2.8) and (2.9) separately.

1. The operator $a_{\beta,1}\mathbf{H}_{0,0}$ is diagonal in all the collective quantum numbers and in k.

2. The operator $a_{\beta,1}V(\theta)$ mixes states both with the same values of κ and n, and with different κ and n, and the matrix elements of this operator do not depend on the angular-momentum quantum number of the state. Therefore, the operator $a_{\beta,1}(\mathbf{H}_{0,0}-V(\theta)-\mathbf{H}_{\text{int}})$ leads to a shift of the energies of the bottoms of the gr and β bands, to renormalization of the moment of inertia, and to deviations from the rigid-rotor formula in the spectrum of these bands.

3. Owing to the axial symmetry, the operator $a_{\beta,2}\mathbf{H}_{0,1}$ mixes states with identical values of the quantum number $k=k_p+k_n$. The dependence of the matrix elements of this operator on the quantum numbers I, K, κ, and n of the initial and final states is completely determined by (2.16). This mixing leads to a shift of the energies of the bottoms of the β and 1^+ bands and to renormalization of the moments of inertia.

4. The operators in Eq. (2.8) mix states with different k [$k(1)-k(2)=2$], i.e., the operator $\mathbf{T}'_\gamma$ allows the states of the gr, β, and $K^\pi=1^+$ bands to mix with states of the γ band. The operators b_1 and b_2 in the Hamiltonian (2.8) change the quantum numbers k by 2 and can connect states of the gr and β bands with states of the γ band. For these operators we use the expression

$$\hat{b}_l=b_l|\gamma\rangle\langle\alpha|+b_l|\alpha\rangle\langle\gamma|,\tag{2.17}$$

where $l=1,2$ and $\alpha=\text{gr},\beta$.

With these assumptions, the nonzero matrix elements of the operators in (2.8) with the wave functions (2.10) are

$$\begin{aligned}\langle IMk'K'\kappa n|\mathbf{T}'_1|IMkK\kappa n\rangle&=[(1+\delta_{K'0}\delta_{k'0})(1+\delta_{K,0}\delta_{k,0})]^{1/2}\{\langle k'|\hat{b}_1|k\rangle\\&\times\delta_{k',k-2}\delta_{K',K-2}[(I+K)(I-K+1)(I+K-1)\\&\times(I-K+2)]^{1/2}+\langle k'|\hat{b}_1^+|k\rangle\delta_{k',k+2}\delta_{K',K+2}[(I-K)\\&\times(I+K+1)(I-K-1)(I+K+2)]^{1/2}\},\end{aligned}\tag{2.18}$$

$$\begin{aligned}\langle IMk'K'\kappa'n'|\hat{\mathbf{T}}'_2|IMkK\kappa n\rangle&=\frac{2i}{\theta_0}[(1+\delta_{K',0}\delta_{k',0})(1+\delta_{K,0}\delta_{k,0})]^{1/2}\left\{\langle k'|\hat{b}_2|k\rangle\right.\\&\times\delta_{k'k-2}\delta_{K'K-1}[(I+K)(I-K+1)]^{1/2}\\&\times\left[\left\langle\kappa'n'\left|\frac{\partial}{\partial x}\right|\kappa n\right\rangle+(k-K-\tfrac{1}{2})\left\langle\kappa'n'\left|\frac{1}{x}\right|\kappa n\right\rangle\right]\\&+\langle k'|\hat{b}_2^+|k\rangle\delta_{k'k+2}\delta_{K'K+1}[(I-K)(I+K+1)]^{1/2}\\&\times\left.\left[\left\langle\kappa'n'\left|\frac{\partial}{\partial x}\right|\kappa n\right\rangle-(k-K+\tfrac{1}{2})\left\langle\kappa'n'\left|\frac{1}{x}\right|\kappa n\right\rangle\right]\right\},\end{aligned}\tag{2.19}$$

$$\langle IMk'K'\kappa'n'|\mathbf{T}'_3|IMkK\kappa n\rangle$$

$$= -\frac{1}{2\theta_0^2}[(1+\delta_{K'0}\delta_{k'0})(1+\delta_{K,0}\delta_{k,0})]^{1/2}\delta_{k',k\pm2}$$
$$\times\left\{\langle\mp k'|\hat{b}_1|k\rangle\left[\left\langle\kappa'n'\left|\frac{\partial^2}{\partial x^2}\right|\kappa n\right\rangle+(\mp k\pm K)^2\right.\right.$$
$$\left.\times\left\langle\kappa'n'\left|\frac{1}{x^2}\right|\kappa n\right\rangle\mp(k-K)\langle\kappa'n'|F(x)|\kappa n\rangle\right]$$
$$+\langle k'|\hat{b}_1^+|\pm k\rangle\left[\left\langle\kappa'n'\left|\frac{\partial^2}{\partial x^2}\right|\kappa n\right\rangle+(\pm k\mp K)^2\right.$$
$$\left.\left.\times\left\langle\kappa'n'\left|\frac{1}{x^2}\right|\kappa n\right\rangle\mp(k-K)\langle\kappa'n'|F(x)|\kappa n\rangle\right]\right\}, \tag{2.20}$$

where

$$F(x)=\left(\frac{\partial}{\partial x}\frac{1}{x}+\frac{1}{x}\frac{\partial}{\partial x}\right).$$

The matrix elements $\langle\kappa'n'|\partial/\partial x|\kappa n\rangle$, $\langle\kappa'n'|1/x|\kappa n\rangle$, and $\langle\kappa'n'|F(x)|\kappa n\rangle$ are easily calculated using (2.14). In general, they are nonzero for any relation between n and n'.

Inclusion of the nondiagonal matrix elements of the inertia operators ($A^{p,n}$) between different internal functions leads to additional renormalization of the moments of inertia of the bands and to deviations from the rigid-rotor expression in the band spectrum. In addition to direct mixing of collective bands constructed on different internal functions, there is also mixing of these bands with $\kappa=1$ bands. The spin dependence of the matrix elements of the Hamiltonian connecting states with $\Delta\kappa=1$ coincides with that for the Hamiltonian of the Coriolis interaction, so that in this model the Coriolis interaction of the β, γ, and $K^\pi=1^+$ bands arises in the same way. The effects of this have been discussed in the first section of this review.

2.3. The method of projection operators in the two-rotor model

The expressions obtained in the preceding section show that the part of the Hamiltonian not included in the operator $\mathbf{H}_{0,0}$ used to construct the basis functions has nondiagonal matrix elements connecting each of the basis states $\Psi(IMkK\kappa n)$ to an infinite number of other states $n\neq n'$. The states which can mix are well separated in energy [see Eq. (2.15)], and so each plays a small role, but to include mixing effects systematically it is necessary to sum the effects associated with the many high-lying states. It is not possible to use perturbation theory directly, owing to the presence of nondiagonal matrix elements in the Hamiltonian matrix which connect low-lying nuclear states, the mixing of which can be arbitrarily strong. A convenient method for including high-lying states is the method of Feshbach projection operators,[88] which split the space of states into two parts.

The Feshbach method

Following Ref. 88, we introduce the operator $\hat{\mathbf{P}}$ which projects onto the space of states of interest (the gr, β, and γ bands):

$$\hat{\mathbf{P}}=\sum_{IM}[|IMgr\rangle\langle IMgr|+|IM\beta\rangle\langle IM\beta|+|IM\gamma\rangle$$
$$\times\langle IM\gamma|]. \tag{2.21}$$

Bearing in mind the application of the scheme to the case where a given number corresponds to several different internal states, we include in the projection operator $\hat{\mathbf{P}}$ two bands with the quantum characteristic $K^\pi=0^+$ (the gr and β bands), differing in their internal properties. All the other states with quantum characteristics $(k=0, K=\kappa=1,n)_{\rm gr}$, $(k=0, K=\kappa=1,n)_\beta$, $(k=2, K=\kappa=1,n)_\gamma$, and $(k=0, K=3, \kappa=1,n)_\gamma$, which we assume to be sufficiently high in energy, are included in the $\mathbf{Q}$ space.

For the projected Hamiltonian we write

$$\mathbf{H}_{pp}=\mathbf{H}^p_{0,0}+\mathbf{P}_0\mathbf{T}'_1\mathbf{P}_0. \tag{2.22}$$

Here we have included $\mathbf{H}^p_{0,0}$, which is diagonal in the basis wave functions Ψ^0, and the part of the operator $\mathbf{T}'_1$ describing the mixing of band states in the $\mathbf{P}$ space (the gr, β, and γ bands).

For the Hamiltonian $\mathbf{H}_{PQ}$ we have

$$\mathbf{H}_{PQ}=\mathbf{P}\mathbf{H}_{0,1}\mathbf{Q}+\mathbf{P}\mathbf{T}'_\beta\mathbf{Q}+\mathbf{P}\mathbf{T}'_2\mathbf{Q}=\mathbf{H}^+_{QP}, \tag{2.23}$$

where

$$\mathbf{H}_{QQ}=\mathbf{H}^0_{0,0}.$$

The operators in (2.23) mix states of $\mathbf{P}$ with the band levels included in the $\mathbf{Q}$ space.

The complete wave function is defined as the sum

$$\Psi=\mathbf{P}\Psi+\mathbf{Q}\Psi=\Phi+\chi. \tag{2.24}$$

The wave function Φ in the $\mathbf{P}$ space has the form

$$\Phi^{IK}=\sum_i\psi_i^{IK}\Phi_i^{IK}, \tag{2.25}$$

where ψ_i^{IK} are the mixing amplitudes of the states IK included in $\mathbf{P}$. The wave function Φ satisfies the equation

$$\tilde{H}\Phi=E\Phi.$$

We assume that the eigenvalues of the low-lying states are considerably smaller than the eigenvalues of the operator $\mathbf{H}_{QQ}$, and that the latter are close to the eigenvalues of $\mathbf{H}^Q_{0,0}=\mathbf{Q}\mathbf{H}_{0,0}\mathbf{Q}$.

Now we can use the approximation

$$\tilde{\mathbf{H}}=\mathbf{H}_{pp}+\mathbf{H}_{PQ}\frac{1}{E-H^Q_{0,0}}\mathbf{H}_{QP}. \tag{2.26}$$

For the matrix elements of $\tilde{\mathbf{H}}$ we then obtain

$$\tilde{\mathbf{H}}_{ii'}=(\mathbf{H}_{PP})_{ii'}+\sum_j(\mathbf{H}_{PQ})_{ij}\frac{1}{E-E_j}(\mathbf{H}_{QP})_{ji'}, \tag{2.27}$$

where j denotes the quantum numbers of the basis functions included in the **Q** space (additional to I and M). For the energy E in the denominator of the second term we take the energy of states of the yrast band.

Using the expressions given in the preceding section for the matrix elements of the Hamiltonian, we obtain the following expression for the matrix:

$$\tilde{\mathscr{H}}=\sum_{i,i'}[\omega_i\delta_{i,i'}+\mathbf{P}_{i,i}I(I+1)], \tag{2.28}$$

where i, $i'=\mathrm{gr}$, β, and γ,

$$\begin{aligned}
\mathbf{P}_{\mathrm{gr,gr}}&=A[1-A_0^2(1+|\langle \mathrm{gr}|a_{\beta,2}|\beta\rangle|^2)]-\frac{4}{A}|\langle \mathrm{gr}|b_2|\gamma\rangle|^2,\\
\mathbf{P}_{\beta,\beta}&=A[1-A_0^2(1+\eta^2|\langle\beta|a_{\beta,2}|\mathrm{gr}\rangle|^2)]\\
&\quad-\frac{4}{A}|\langle\beta|b_2|\gamma\rangle|^2,\\
\mathbf{P}_{\gamma,\gamma}&=A\left[1-A_0^2\sum{}'\right]-\frac{2}{A}[|\langle \mathrm{gr}|b_2|\gamma\rangle|^2+|\langle\beta|b_2|\gamma\rangle|^2]\\
&\quad\times\left[1-\frac{2}{I(I+1)}\right],\\
\mathbf{P}_{\beta,\mathrm{gr}}&=A[\langle \mathrm{gr}|a_{\beta,1}|\beta\rangle-A_0^2\langle \mathrm{gr}|a_{\beta,2}|\beta\rangle(1+\eta)],\\
\mathbf{P}_{\mathrm{gr},\gamma}&=\sqrt{2}[\langle \mathrm{gr}|b_1|\gamma\rangle-A_0\langle \mathrm{gr}|a_{\beta,2}|\beta\rangle\\
&\quad\times\langle\beta|b_2|\gamma\rangle]\left[1-\frac{2}{I(I+1)}\right]^{1/2},
\end{aligned} \tag{2.29}$$

$$\begin{aligned}
\mathbf{P}_{\beta,\gamma}&=\sqrt{2}[\langle\beta|b_1|\gamma\rangle-A_0\eta\langle\beta|a_{\beta,2}|\mathrm{gr}\rangle\\
&\quad\times\langle \mathrm{gr}|b_2|\gamma\rangle]\left[1-\frac{2}{I(I+1)}\right]^{1/2},
\end{aligned}$$

$A=\frac{1}{2}\omega\theta_0^2$ is the inertia parameter of the core,

$$A_0=(A_p^0-A_n^0)/(A_p^0+A_n^0),$$

$$\sum{}'=5+\sum_{n=1}^{\infty}\frac{4}{(2n+1)(n+1)}\approx 6.543,$$

and ω_i are the principal band energies. We note that in the diagonal terms all quantities independent of the spin I are included in ω_i.

Electromagnetic transitions

Let us calculate the matrix element of the multipole operator $\hat{m}(\lambda,\mu)$. In this model the matrix element of the operator $\hat{m}(\lambda,\mu)$ between the wave functions (2.24) has the form

$$\begin{aligned}
&\langle\Psi_1^{I_1}|\hat{m}(\lambda,\mu)|\Psi_2^{I_2}\rangle\\
&\quad=\langle\Phi_1^{I_1}|\hat{m}(\lambda,\mu)|\Phi_2^{I_2}\rangle+\langle\Phi_1^{I_1}|\hat{m}(\lambda,\mu)|\chi_2^{I_2}\rangle\\
&\qquad+\langle\chi_1^{I_1}|\hat{m}(\lambda,\mu)|\Phi_2^{I_2}\rangle+\langle\chi_1^{I_1}|\hat{m}(\lambda,\mu)|\chi_2^{I_2}\rangle,
\end{aligned} \tag{2.30}$$

where

$$\langle\Phi_1^{I_1}|\hat{m}(\lambda,\mu)|\Phi_2^{I_2}\rangle=\sum_{ii'}\psi_i^{I_1 1}\psi_{i'}^{I_2 2}\langle\chi_i^{I_1 1}|\hat{m}(\lambda,\mu)|\Phi_{1'}^{I_2 2}\rangle, \tag{2.31}$$

$$\langle\Phi_1^{I_1}|\hat{m}(\lambda,\mu)|\chi_2^{I_2}\rangle=\sum_j\frac{\Sigma_{ii'}\psi_i^{I_1 1}\psi_{i'}^{I_2 2}\langle\Phi_i^{I_1 1}|\hat{m}(\lambda,\mu)|\Phi_j^{I_2 2}\rangle\langle\Phi_j^{I_2}|\mathbf{H}_{QP}|\Phi_{i'}^{I_2 2}\rangle}{E-E_j}, \tag{2.32}$$

$$\langle\chi_1^{I_1}|\hat{m}(\lambda,\mu)|\Phi_2^{I_2}\rangle=\sum_j\frac{\Sigma_{ii'}\psi_i^{I_1 1}\psi_{i'}^{I_2 2}\langle\Phi_i^{I_1 1}|\mathbf{H}_{PQ}|\Phi_j^{I_1}\rangle\langle\Phi_j^{I_1}|\hat{m}(\lambda,\mu)|\Phi_{i'}^{I_2 2}\rangle}{E-E_j}, \tag{2.33}$$

$$\langle\chi_1^{I_1}|\hat{m}(\lambda,\mu)|\chi_2^{I_2}\rangle=\sum_{jj'}\frac{\Sigma_{ii'}\psi_i^{I_1 1}\psi_{i'}^{I_2 2}\langle\Phi_i^{I_1 1}|\mathbf{H}_{PQ}|\Phi_j^{I_1}\rangle\langle\Phi_j^{I_1}|\hat{m}(\lambda,\mu)|\Phi_{j'}^{I_2}\rangle\langle\Phi_{j'}^{I_2}|\mathbf{H}_{QP}|\Phi_{i'}^{I_2 2}\rangle}{(E-E_j)\cdot(E-E_{j'})}. \tag{2.34}$$

Here the summation runs over the indices i and j of the states of the **P** and **Q** spaces, respectively.

We use the multipole operator of Ref. 40 for the magnetic dipole transition. The isoscalar operator $M_0(M1,\mu)$ in Ref. 40 contributes only to the static magnetic moment of the nucleus in the state with spin I (Refs. 40 and 86). The isovector magnetic dipole moment $M_\theta(M1,\mu)$ also contributes to the static magnetic moment and does not change the internal state of the nucleus, i.e., it is diagonal in χ_k. Therefore, there is no $M1$ transition between the eigenfunctions of $\mathbf{H}_{0,0}^P$. According to Ref. 40, the nonzero matrix elements of $M_\theta(M1,\mu)$ between functions of **P** space ($i\equiv kK,\kappa=0,n=0$) and functions of **Q** space ($j\equiv k,K\pm1,\kappa=1,n'$) are given by

$$\begin{aligned}
&\langle I_2M_2k,K\pm1,\kappa+1,n_2|m_\theta(M1,\mu)|I_1M_1kK\kappa n_1\rangle\\
&\quad=\pm\frac{i}{\theta_0}\left(\frac{3}{16\pi}\right)^{1/2}(g_p-g_n)\frac{e\hbar}{2mc}\\
&\qquad\times\left[\frac{1+\delta_{K,0}\delta_{k,0}}{2}\right]^{1/2}\left(\frac{2I_1+1}{2I_2+1}\right)^{1/2}C^{I_2M_2}_{I_1M_1,10}C^{I_2K\pm1}_{I_1K,1\pm1}\\
&\qquad\times\left\{\frac{n_1\mp(k-K)+1}{(n_1+\kappa+1)^{1/2}}\delta_{n_1n_2}+(\pm K\mp k-\kappa)\right.\\
&\qquad\left.\times\left[\frac{n_2!(n_1+\kappa)!}{n_1!(n_2+\kappa+1)!}\right]^{1/2}+\sqrt{n_1}\delta_{n_2n_1-1}\right\}.
\end{aligned} \tag{2.35}$$

Inclusion of the mixing of the bands of the **P** and **Q**

spaces in the Feshbach formalism described above leads to the appearance of $M1$ transitions between the states of **P** space, i.e., the matrix elements (2.32) and (2.33) are nonzero. An explicit expression for $\langle \Phi_i^{I_1 1} | \hat{m}(M1) | \Phi_j^{I_2} \rangle$ is obtained by substituting (2.35) into (2.32) and (2.33):

$$\langle \Psi_{\rm gr}^{I_f} || M_\theta(M1;\mu) || \Psi_K^{I_i} \rangle$$
$$= -\left(\frac{3}{16\pi}\right)^{1/2} (g_p - g_n)\left(\frac{e\hbar}{2mc}\right)$$
$$\times \sqrt{2I_i+1} \sum_{i,i'} \psi_i^{I_f \rm gr} \psi_{i'}^{I_i K} \cdot a_{i,i'} \qquad (2.36)$$

$$a_{\rm gr,gr} = a_{\beta,\beta} = \frac{A_0}{\sqrt{2}} [\sqrt{I_i(I_i+1)} C_{I_i 1;1-1}^{I_f 0} - \sqrt{I_f(I_f+1)} C_{I_i 0;11}^{I_f 1}],$$

$$a_{\gamma,\gamma} = \frac{A_0}{2\sqrt{2}} [\sqrt{I_i(I_i+1)-2} C_{I_i 1;11}^{I_f 2} - \sqrt{I_f(I_f+1)-2} C_{I_i 2;1-1}^{I_f 1} - 3\sqrt{I_f(I_f+1)-6} C_{I_i 2;11}^{I_f 3} + 3\sqrt{I_i(I_i+1)-6} C_{I_i 3;1-1}^{I_f 2}],$$

$$a_{\rm gr,\beta} = \frac{A_0}{\sqrt{2}} \langle {\rm gr}|a_{\beta,2}|\beta\rangle [\eta \cdot \sqrt{I_i(I_i+1)} C_{I_i 1;1-1}^{I_f 0} - \sqrt{I_f(I_f+1)} C_{I_i 0;11}^{I_f 1}],$$

$$a_{\beta,\rm gr} = \frac{A_0}{\sqrt{2}} \langle {\rm gr}|a_{\beta,2}|\beta\rangle [\sqrt{I_i(I_i+1)} C_{I_i 1;1-1}^{I_f 0} - \eta \cdot \sqrt{I_f(I_f+1)} C_{I_i 0;11}^{I_f 1}],$$

$$a_{\alpha,\gamma} = \frac{\langle \alpha|b_2|\gamma\rangle}{A} [\sqrt{I_i(I_i+1)-2} C_{I_i 1;1-1}^{I_f 0} + \sqrt{I_f(I_f+1)} C_{I_i 2;1-1}^{I_f 1}],$$

$$a_{\gamma,\alpha} = -\frac{\langle \alpha|b_2|\gamma\rangle}{A} [\sqrt{I_i(I_i+1)} C_{I_i 1;11}^{I_f 2} + \sqrt{I_f(I_f+1)-2} C_{I_i 0;11}^{I_f 1}],$$

where $\alpha = {\rm gr}, \beta$; g_p and g_n are the gyromagnetic ratios of the proton and neutron subsystems.

Equation (2.36) for the reduced probabilities of $M1$ transitions from odd states of the γ band have the form

$$B(M1; I \underset{\gamma}{\to} (I-1)_K) = \frac{3}{16\pi} (g_p - g_n)^2 \left(\frac{e\hbar}{2mc}\right)^2 \left(\frac{I+2}{2I+1}\right) \times \left\{ \frac{\sqrt{2}}{A} [\langle {\rm gr}|b_2|\gamma\rangle \psi_{\rm gr}^{I-1K} + \langle \beta|b_2|\gamma\rangle \psi_\beta^{I-1K}] \sqrt{I^2-1} + 4A_0 \sqrt{\frac{I-2}{I}} \psi_\gamma^{I-1K} \right\}^2 (\psi_\gamma^{I\gamma})^2. \qquad (2.37)$$

For the magnetic moment of the collective states we have

$$\mu = g_R(I) \cdot I, \qquad (2.38)$$

where

$$g_R(I) = \frac{1}{2}(g_p+g_n) - \frac{1}{2}(g_p-g_n) \sum_{i,i'} \psi_i^{IK} \psi_{1'}^{IK} a_{i,i'},$$

$$a_{\rm gr,gr} = a_{\beta,\beta} = A_0,$$

$$a_{\gamma,\gamma} = A_0[1 - 8/I(I+1)],$$

$$a_{\beta,\rho} = a_{{\rm gr},\beta} = A_0 \langle \beta|a_{\beta,2}|{\rm gr}\rangle (1+\eta),$$

$$a_{{\rm gr},\gamma} = a_{\gamma,{\rm gr}} = \frac{\sqrt{2}}{A} \langle {\rm gr}|b_2|\gamma\rangle [1 - 2/I(I+1)]^{1/2},$$

$$a_{\gamma,\beta} = a_{\beta,\gamma} = \frac{\sqrt{2}}{A} \langle \beta|b_2|\gamma\rangle [1 - 2/I(I+1)]^{1/2}. \qquad (2.39)$$

An additional parameter $\frac{1}{2}(g_p+g_n)$ determined from experiment arises in the description of the g_R factor of the states of the **P** space.

In a similar way we obtain the expression for the reduced $E2$-transition probability, introducing the following expression for the quadrupole electric-moment operator of the nucleus:

$$M(E2,\mu) = \sum_\nu D_{\mu\nu}^2(\Omega) m'_{2\nu} + \left(\frac{5}{16\pi}\right)^{1/2} D_{\mu 0}^2(\Omega) Q_0, \qquad (2.40)$$

where

$$m'_{2\nu} = m_{|\nu|}(|\nu\rangle\langle {\rm gr}| + |{\rm gr}\rangle\langle \nu|). \qquad (2.41)$$

Here $m'_{2\nu}$ are determined in the coordinate frame attached to the nucleus, Q_0 is the internal quadrupole moment of the nucleus, and $|\nu\rangle = |\beta\rangle, |\gamma\rangle$. The isovector part of the operator (2.40) will be discussed later on.

Equation (2.31) describes the probabilities of $E2$ transitions between states of the gr, β, and γ bands included in **P** space. The reduced matrix element of the $E2$ transition calculated from (2.31) using the multipole operator (2.40) has the form

$$\langle \Phi_{\rm gr}^{I_2} || M(E2) || \Phi_K^{I_1} \rangle$$
$$= \sqrt{2I_1+1} \left\{ \left(\frac{5}{16\pi}\right)^{1/2} Q_0 \left[\psi_{\rm gr}^{I_2 \rm gr} \psi_{\rm gr}^{I_1 K} C_{I_1 0;20}^{I_2 0} + \sum_i \psi_{K_i}^{I_2 \rm gr} \psi_{K_i}^{I_1 K} C_{I_1 K_i;20}^{I_2 K_1} \right] + \sqrt{2} \left[\psi_{\rm gr}^{I_2 \rm gr} \sum_i \frac{m_i \psi_i^{I_1 K}}{\sqrt{1+\delta_{K_i,0}}} \times C_{I_1 K_i;2-K_i}^{I_2 0} + \psi_{\rm gr}^{I_1 K} \sum_i \frac{m_i \psi_i^{I_2 \rm gr}}{\sqrt{1+\delta_{K_i,0}}} C_{I_1 0;2K_i}^{I_2 K_i} \right] \right\}. \qquad (2.42)$$

This equation describes the ground-state component of the probability of transitions between states of the **P** space, and the matrix elements (2.32) and (2.33) of the quadrupole operator are equal to zero.

2.4. The effect of giant angular resonances on the electromagnetic characteristics of low-lying levels

The calculations were carried out for isotopes of Er. The model parameters were chosen as follows. The principal energies of the gr and β bands were taken from experiment. The inertia parameter A was determined using the experimental energy $E_{\rm gr}^{\rm exp}(I=2)$ of the ground-state band. The parameters A_0 and ω_γ were determined from the experimental data on the energies of states of the γ band with odd I.

The mixing of states leads to strong violation of the rules of the adiabatic theory for the transition branching. The mixing effects are most simply interpreted by using the wave functions of first-order perturbation theory in the band-coupling parameters:[89]

$$
\begin{aligned}
|\mathrm{gr}\,IM\rangle &= |\mathrm{gr}(K=0)IM\rangle - \mathscr{E}_{\mathrm{gr},\beta} I(I+1)|\beta(K=0)IM\rangle \\
&\quad - \mathscr{E}_{\mathrm{gr},\gamma}\sqrt{2}\tilde{I}|\gamma(K=2)IM\rangle, \\
|\beta IM\rangle &= |\beta(K=0)IM\rangle + \mathscr{E}_{\mathrm{gr},\beta} I(I+1)|\mathrm{gr}(K=0)IM\rangle \\
&\quad - \mathscr{E}_{\beta,\gamma}\sqrt{2}\tilde{I}|\gamma(K=2)IM\rangle, \qquad (2.43) \\
|\gamma IM\rangle &= |\gamma(K=2)IM\rangle + \sqrt{2}\tilde{I}[\mathscr{E}_{\mathrm{gr},\gamma}|\mathrm{gr}(K=0)IM\rangle \\
&\quad + \mathscr{E}_{\beta,\gamma}|\beta(K=0)IM\rangle],
\end{aligned}
$$

where

$$
\mathscr{E}_{\mathrm{gr},\beta} = \frac{A\langle \mathrm{gr}|a_{\beta,1}|\beta\rangle}{\omega_\beta}, \quad \mathscr{E}_{\alpha,\gamma} = \frac{\langle \alpha|b_1|\gamma\rangle}{\omega_\gamma - \omega_\alpha},
$$

$$
\tilde{I} = I(I+1)\left[1 - \frac{2}{I(I+1)}\right]^{1/2}.
$$

Using Eq. (2.40) for the matrix element of the operator corresponding to the quadrupole moment of the charge distribution, we arrive at the expression

$$
\begin{aligned}
&\langle \mathrm{gr}I_2||m(E2)||\gamma I_1\rangle \\
&= \langle \mathrm{gr}(K=0)I_2||m(E_2)||\gamma(K=2)I_1\rangle \\
&\quad + \sqrt{2}\tilde{I}_1\left\{\mathscr{E}_{\mathrm{gr},\gamma} + \mathscr{E}_{\beta,\gamma}\cdot\left(\frac{16\pi}{5}\right)^{1/2}\frac{m_\beta}{Q_0}\right\} \\
&\quad \times \langle \mathrm{gr}(K=0)I_2||\hat{m}(E2)||\mathrm{gr}(K=0)I_1\rangle - \sqrt{2}\tilde{I}_1\mathscr{E}_{\mathrm{gr},\gamma} \\
&\quad \times \langle \gamma(K=2)I_2||m(E2)||\gamma(K=2)I_1\rangle. \qquad (2.44)
\end{aligned}
$$

The ratio of the reduced probabilities of $E2$ transitions from the γ-vibrational band is

$$
R_{I\gamma} = \frac{B(E2;I_{i\gamma}\to I_{f\mathrm{gr}})}{B(E2;I_{i\gamma}\to I'_{f\mathrm{gr}})}
$$

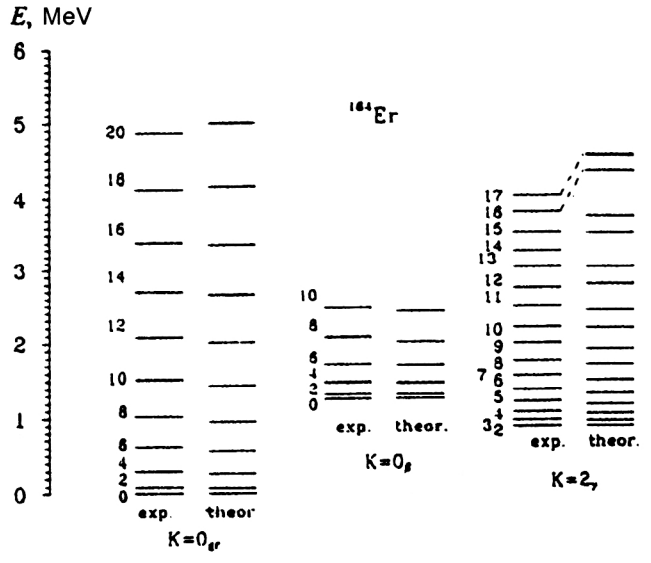

FIG. 15. Comparison of the experimental and theoretical energies of positive-parity states for ^{164}Er.

$$
= \left| \frac{C^{I_f 0}_{I_i 2;2-2} + \dfrac{Z_\gamma(0)}{\sqrt{24}}\tilde{I}_i C^{I_f 0}_{I_i 0;20} - \dfrac{Z_\gamma(2)}{\sqrt{24}}\tilde{I}_f C^{I_f 2}_{I_i 2;20}}{C^{I'_f 0}_{I_i 2;2-2} + \dfrac{Z_\gamma(0)}{\sqrt{24}}\tilde{I}_i C^{I'_f 0}_{I_i 0;20} - \dfrac{Z_\gamma(2)}{\sqrt{24}}\tilde{I}_f C^{I'_f 2}_{I_i 2;20}} \right|^2 . \qquad (2.45)
$$

The branching of transitions from γ bands is completely determined by two spin-independent parameters:

$$
\begin{aligned}
Z_\gamma(2) &= \mathscr{E}_{\mathrm{gr},\gamma}\sqrt{24}\,\frac{\sqrt{5/16\pi}\,Q_0}{m_\gamma}, \\
Z_\gamma(0) &= \left\{1 + \frac{\mathscr{E}_{\beta,\gamma}}{\mathscr{E}_{\mathrm{gr},\gamma}}\left(\frac{16\pi}{5}\right)^{1/2}\frac{m_\beta}{Q_0}\right\} Z_\gamma(2).
\end{aligned} \qquad (2.46)
$$

The spin dependence of the reduced transition probabilities calculated in this manner coincides with that for the case of two mixing bands possessing different internal quadrupole moments.[47] The factor

$$
1 + \frac{\mathscr{E}_{\beta,\gamma}}{\mathscr{E}_{\mathrm{gr},\gamma}}\left(\frac{16\pi}{5}\right)^{1/2}\frac{m_\beta}{Q_0}
$$

renormalizes the internal quadrupole moment of the ground-state band.

The values of the matrix elements $\langle \mathrm{gr}|b_1|\gamma\rangle$ and $\langle \beta|b_1|\gamma\rangle$ describing the direct mixing of the gr, β, and γ bands are found from Eq. (2.46). Here the parameters $Z_\gamma(K)$ are determined by (2.45) with the experimental data on the ratios of reduced probabilities of $E2$ transitions from the γ-vibrational band. The parameters m_β and m_γ are found from (1.12) and (1.13), using the experimental data on $B(E2)$ for ^{164}Er (Ref. 4). The free parameters of the model are η, $\langle \mathrm{gr}|a_{\beta,2}|\beta\rangle$, $\langle \mathrm{gr}|b_2|\gamma\rangle$, and $\langle \beta|b_2|\gamma\rangle$, which were found by the method of least squares by requiring the best agreement between the theoretical energy spectrum and experiment. The calculated spectra of collective positive-parity states for the isotopes ^{164,166,168}Er are shown in Figs. 15, 16,

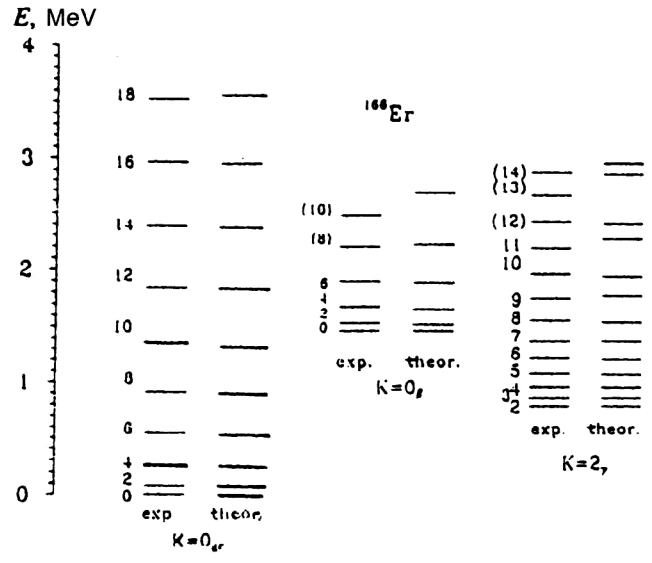

FIG. 16. Comparison of the experimental and theoretical energies of positive-parity states for ^{166}Er.

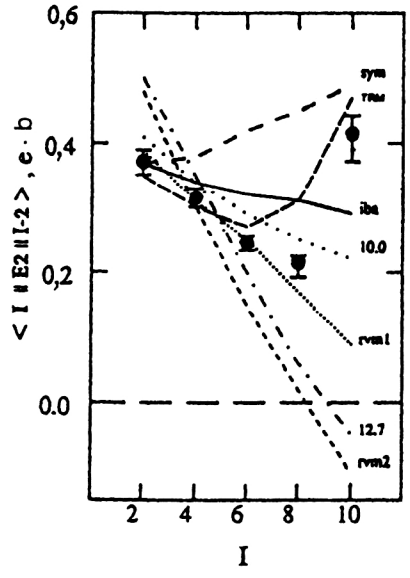

FIG. 18. Spin dependence of the experimental and calculated values of the $I_\gamma \to (I-2)_{gr}$ matrix elements in ^{166}Er. The matrix elements calculated using the following models are given: sym—the symmetric rotor model, the asymmetric rotor model[93] (10.0 and 12.7, calculated with the values $\gamma = 10°$ and 12.7°, respectively), rvm—the rotational-vibrational model,[94] iba—the interacting-boson approximation),[95] and TRM—the two-rotor model.[77]

and 17, respectively. We see from Fig. 15 that theory and experiment disagree for spins $I \geqslant 14$ in the γ band of ^{164}Er. This is certainly related to the fact that the **P** space does not include the following experimentally observed bands:

(a) Bands with $K^\pi = 0^+$ with principal energies 1.698, 1.766, 2.173, and 2.185 MeV (Refs. 4 and 5).

(b) The aligned band beginning at spin $I = 12$, which intersects the ground-state band and leads to backbending of the moment of inertia.

We have restricted our study to the properties of low-lying excited levels. The neglected bands do not strongly affect the characteristics of these levels.

The reduced probabilities of $E2$ transitions from the γ-vibrational band were calculated by (2.42) with the values $m_0 = \pm 0.10$ b, $m_2 = \pm 0.27$ b, and $Q_0 = 7.42$ b determined above (Ref. 4).

In Table XV we give the values of $B(E2)$ for the γ band of ^{168}Er and compare them with experiment[90] and with the theoretical values of $B(E2)$ calculated using IBA2.[91] We see from this table that the values of $B(E2)$ calculated in our model are in better agreement with experiment.

Fahlander *et al.*[92] experimentally determined the values of the matrix elements of $E2$ transitions between positive-parity states in ^{166}Er, where the matrix element $\langle (I-2)\gamma \| E2 \| I_{gr} \rangle$ depends nonmonotonically on the angular momentum I. This behavior of the matrix element is successfully described by our model (see Fig. 18). Various other models,[92] including one with Coriolis mixing of bands via $\Delta K = 1$, cannot describe it, although the latter model reproduces the ratios of probabilities of $E2$ transitions from states

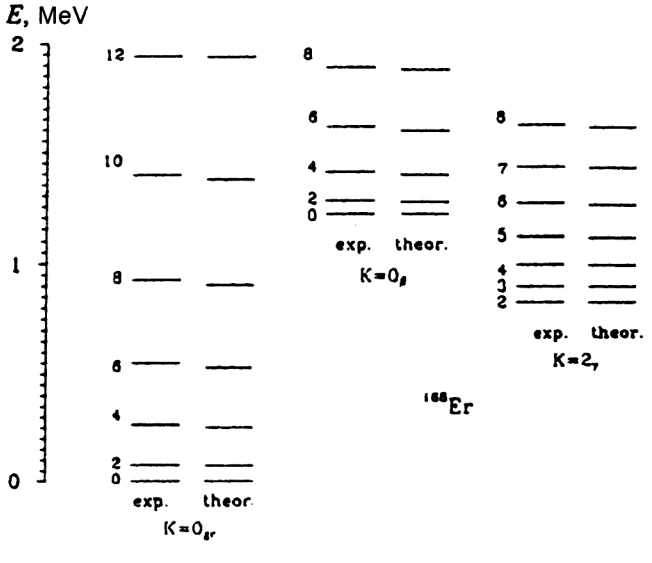

FIG. 17. Comparison of the experimental and theoretical energies of positive-parity states for ^{168}Er.

TABLE XV. Values of $B(E2)$ for $\gamma \to$ gr transitions in ^{168}Er.

Transitions	$B(E2)$ (e^2 b^2)		
	Ref. 90	Ref. 91	TRM (Ref. 77)
$2_\gamma \to 0_{gr}$	0.028(2)	0.028	0.026
$\to 2_{gr}$	0.051(7)	0.066	0.046
$\to 4_{gr}$	0.0035(5)	0.0025	0.0035
$3_\gamma \to 2_{gr}$	0.046(13)	0.054	0.047
$\to 4_{gr}$	0.030(8)	0.041	0.029
$4_\gamma \to 2_{gr}$	0.0094(14)	0.0068	0.012
$\to 4_{gr}$	0.048(7)	0.080	0.055
$\to 6_{gr}$	0.0065(10)	0.0039	0.0089
$5_\gamma \to 4_{gr}$	0.027(4)	0.036	0.036
$\to 6_{gr}$	0.034(6)	0.054	0.041
$6_\gamma \to 4_{gr}$	0.005(1)	0.0021	0.0079
$\to 6_{gr}$	0.043(7)	0.079	0.055

TABLE XVI. Matrix elements of $E2$ transitions between positive-parity states in ^{166}Er.

Transitions	Exp. (Ref. 92)	Theory	
		IBA1 (Ref. 92)	TRM (Ref. 77)
$2_{gr}\to 0_{gr}$	$2.28^{+0.11}_{-0.11}$	2.40	2.33
$4_{gr}\to 2_{gr}$	$3.86^{+0.12}_{-0.12}$	3.84	3.75
$6_{gr}\to 4_{gr}$	$4.70^{+0.19}_{-0.14}$	4.79	4.76
$8_{gr}\to 6_{gr}$	$5.81^{+0.20}_{-0.20}$	5.52	5.60
$10_{gr}\to 8_{gr}$	$6.47^{+0.25}_{-0.25}$	6.08	6.35
$12_{gr}\to 10_{gr}$	$7.00^{+0.30}_{-0.30}$	6.51	7.01
$14_{gr}\to 12_{gr}$	$8.15^{+0.41}_{-0.86}$	6.81	7.58
$16_{gr}\to 14_{gr}$	$7.66^{+2.04}_{-2.18}$	6.98	8.09
$2_{\gamma}\to 0_{gr}$	$0.372^{+0.019}_{-0.019}$	0.37	0.36
$4_{\gamma}\to 2_{gr}$	$0.315^{+0.016}_{-0.016}$	0.34	0.30
$6_{\gamma}\to 4_{gr}$	$0.244^{+0.012}_{-0.012}$	0.32	0.27
$8_{\gamma}\to 6_{gr}$	$0.214^{+0.011}_{-0.022}$	0.31	0.30
$10_{\gamma}\to 8_{gr}$	$0.416^{+0.027}_{-0.044}$	0.29	0.45
$2_{gr}\to 2_{gr}$	$-2.33^{+0.19}_{-0.12}$	−2.87	−2.78
$4_{gr}\to 4_{gr}$	$-2.12^{+0.34}_{-0.16}$	−3.61	−3.53
$6_{gr}\to 6_{gr}$	$-4.03^{+0.25}_{-0.20}$	−4.19	−4.17
$8_{gr}\to 8_{gr}$	$-4.74^{+0.24}_{-0.47}$	−4.62	−4.72
$10_{gr}\to 10_{gr}$	$-6.78^{+0.45}_{-0.95}$	−4.92	−5.25
$4_{\gamma}\to 2_{\gamma}$	$2.60^{+0.13}_{-0.13}$	2.28	2.38
$6_{\gamma}\to 4_{\gamma}$	$4.44^{+0.22}_{-0.22}$	3.80	4.01
$8_{\gamma}\to 6_{\gamma}$	$5.28^{+0.26}_{-0.26}$	4.69	5.02
$10_{\gamma}\to 8_{\gamma}$	$5.65^{+0.28}_{-0.28}$	5.29	5.84
$12_{\gamma}\to 10_{\gamma}$	$6.00^{+0.77}_{-1.20}$	5.29	6.57
$2_{\gamma}\to 2_{gr}$	$0.518^{+0.026}_{-0.026}$	0.49	0.49
$4_{\gamma}\to 4_{gr}$	$0.727^{+0.036}_{-0.036}$	0.71	0.73
$6_{\gamma}\to 6_{gr}$	$0.834^{+0.042}_{-0.042}$	0.83	0.89
$8_{\gamma}\to 8_{gr}$	$0.969^{+0.048}_{-0.048}$	0.92	1.01
$2_{\gamma}\to 4_{gr}$	$0.161^{+0.026}_{-0.022}$	0.13	0.14
$4_{\gamma}\to 6_{gr}$	$0.326^{+0.016}_{-0.041}$	0.27	0.27
$6_{\gamma}\to 8_{gr}$	$0.33^{+0.31}_{-0.30}$	0.39	0.31
$8_{\gamma}\to 10_{gr}$	$0.37^{+0.18}_{-0.30}$	0.49	0.18

of the γ band well (see Table III). In Table XVI we give the matrix elements of $E2$ transitions for ^{166}Er calculated in this model and compare them with the IBA1 calculations and with experiment.[92]

In Tables II–IV we give the theoretical values of the ratios of the reduced $E2$-transition probabilities for ^{164,166,168}Er along with the experimental data and the values calculated using the Alaga formula. We see from this table that the model satisfactorily describes the deviation of the ratios of the reduced $E2$-transition probabilities from the Alaga rule using the same internal quadrupole moment Q_0 for the ground-state ($K=0$) and γ ($K=2$) bands, in contrast to Ref. 47, where $Q_0(K=0)\neq Q_0(K=2)$. We should note that $B(E2)$ was calculated with a single set of m_K and Q_0 for all the Er isotopes.

The multipole-mixture coefficients δ were calculated. In Tables V and VI we compare the values of δ found in this model with the experimental values for ^{164,168}Er. The best value of δ was obtained for

$$B(M1;00_{gr}\to 1^+1)=\frac{\omega_1}{2A}\frac{3}{16\pi}(g_p-g_n)^2.$$

Here $B(M1;00_{gr}\to 1^+1)=0.8\mu_n^2$ for ^{164}Er and $1.75\mu_n^2$ for ^{166,168}Er at the fixed value $\omega_1=3$ MeV. The IBA2 calculations for ^{168}Er give $B(M1)=1.5\mu_n^2$ (Ref. 96). Experiment[22,23] for ^{168}Er gives $B(M1)=1.5\mu_n^2$ and $\omega_1=3.4$ MeV. The (e,e') and nuclear-resonance fluorescence experiments give[97,98] $(2.50\pm0.21)\mu_n^2$ and $(2.20\pm0.16)\mu_n^2$, respectively, for the sum of transitions $\Sigma B(M1)\uparrow(E_x\leq 4\text{ MeV})$ in ^{168}Er. They are always larger than our estimates $B(M1;0^+0\to 1^+1)=1.75\mu_n^2$, since here we have not evaluated transitions from the states $(k=0,K=\kappa=1,n)_\beta$ and $(k=2,K=1,\kappa=1,n)_\gamma$ to the ground state. However, their contributions are taken into account in the calculations of the multipole-mixture coefficients δ.

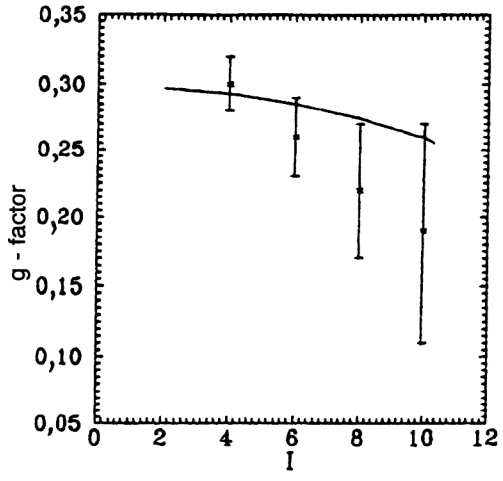

FIG. 19. Comparison of the calculated and experimental values[100] of the g_R factor for states of the ground-state band of ^{166}Er.

The results of these studies lead to the following conclusions.

1. Mixing of the **P** and **Q** spaces leads to renormalization of the moments of inertia of the bands included in the **P** space. This is reflected in the eigenfunctions of the states and therefore significantly affects the values of electromagnetic transitions between the states of the **P** space. The deviations of the ratios $R_{I\gamma}$ from the Alaga rule are mainly related to the mixing of states of the **P** space, and also to the mixing of states of the **P** and **Q** spaces.

2. The presence of giant-angular-resonance components in the wave functions of β- and γ-vibrational states leads to $M1$ transitions from them to states of the ground-state band.

3. The multipole-mixture coefficients δ for transitions from the γ band decrease in absolute value with increasing angular momentum I.

4. From the condition of best reproduction of the coefficients δ^{exp} of the low-lying levels we have $B(M1;00_{gr}\to 1^+1)=0.8\mu_n^2$ for ^{164}Er and $\approx 1.75\mu_n^2$ for ^{166,168}Er at the fixed value $\omega_1=3$ MeV.

In Fig. 19 we show the calculated values of the g_R factor for the ground-state band of ^{166}Er along with the experimental data.[100] We see that the model describes the decrease of g_R with increasing angular momentum, which is a manifestation of nonadiabaticity in the states of the ground-state band. This behavior of g_R cannot be described using the

approach of Refs. 84 and 85. Nonadiabaticity is not manifested in the ground-state band in intraband $E2$ transitions (see Table XIII), and it is manifested in the magnetic characteristics of the states. This indicates that the states of the gr band mix with the levels of bands having large matrix elements of $M1$ transitions, which are giant-angular- resonance states.

CONCLUSION

In this review we have focused on phenomenological models and methods which allow the description of a large amount of experimental data on the deviations of the properties of positive-parity states in even–even deformed nuclei from the regularities of the adiabatic theory. In particular, we have demonstrated the possibility of studying the effects of mixing of adiabatic bands by using identical fundamental parameters (the moments of inertia and the internal quadrupole moments).

We have proposed an improved version of the two-rotor model, where the inclusion of the internal states of the proton and neutron subsystems leads to the prediction that there are giant-angular-resonance excitations above states having different internal configurations. We have shown that the mixing of $\Delta K=1$ states is determined by the matrix element of the operator $\mathbf{S}=\mathbf{I}_p-\mathbf{I}_n$ having the same dependence on the quantum numbers I and K as the matrix element of the Coriolis interaction. This version of the model has been developed by using the Feshbach formalism for splitting the space of states into two subspaces. We have studied the spectrum of the system and have shown that in nuclei with large neutron excess the effects of coupling between the rotation of the nucleus as a whole and the relative displacements of the neutron and proton components lead to strong renormalizations of the nuclear moment of inertia, and also of the magnetic moments of the states of various bands. We have shown that the presence of components of giant-angular-resonance states in the wave functions of vibrational states leads to $M1$ transitions to states of the ground-state band.

In summary, it can be stated that the models and methods used in this review allow the systematic inclusion of the effects of mixing of rotational bands in even–even deformed nuclei, which, in particular, makes it possible to: (1) describe the anomalous behavior of the reduced $E0$-, $E2$-, and $M1$-transition probabilities and also the g_R factor with increasing total spin of the nucleus, and (2) predict a number of new characteristics of excited nuclear states.

The authors would like to thank their colleagues Ch. Briançon, E. P. Grigor'ev, K. Ya. Gromov, V. G. Kalinnikov, R. Kulessa, V. M. Mikhaĭlov, I. A. Mitropol'skiĭ, R. G. Nazmitdinov, V. O. Nesterenko, R. A. Niyazov, A. A. Okhunov, V. G. Solov'ev, C. Fahlander, A. Kh. Kholmatov, and É. Kh. Yuldashbaeva for their interest in the study and discussion of the results.

[1] A. Bohr and B. R. Mottelson, *Nuclear Structure*, Vols. 1 and 2 (Benjamin, New York, 1969, 1975) [Russ. transl., Mir, Moscow, 1971, 1977].
[2] V. G. Soloviev (Solov'ev), *Theory of Complex Nuclei* (Pergamon Press, Oxford, 1976) [Russ. original, Nauka, Moscow, 1971].
[3] E. P. Grigor'ev and V. G. Solov'ev, *Structure of Even Deformed Nuclei* [in Russian] (Moscow, Nauka, 1974).
[4] R. B. Begzhanov, V. M. Belen'kiĭ, I. I. Zalyubovskiĭ, and A. V. Kuznechenko, *Handbook of Nuclear Physics*, Vols. 1–2 [in Russian] (FAN, Tashkent, 1989).
[5] V. M. Belen'kiĭ and E. P. Grigor'ev, *Nuclear Structure* [in Russian] (Énergoatomizdat, Moscow, 1987).
[6] P. C. Sood, D. M. Headly, and R. K. Sheline, At. Data Nucl. Data Tables **47**, 89 (1991).
[7] E. N. Shurshikov and N. V. Timofeeva, Nucl. Data Sheets **67**, 45 (1992).
[8] B. Singh, Nucl. Data Sheets **75**, 199 (1995).
[9] Ch. Briançon and I. N. Mikhaĭlov, Fiz. Élem. Chastits At. Yadra **13**, 245 (1982) [Sov. J. Part. Nucl. **13**, 101 (1982)].
[10] S. M. Harris, Phys. Rev. B **138**, 509 (1965).
[11] D. R. Inglis, in *Problems in Modern Physics* [in Russian] (IL, Moscow, 1956), No. 1, p. 139.
[12] D. R. Inglis, in *Problems in Modern Physics* [in Russian] (IL, Moscow, 1956), No. 1, p. 152.
[13] V. M. Mikhaĭlov, Izv. Akad. Nauk SSSR, Ser. Fiz. **30**, 1334 (1966) [Bull. Acad. Sci. USSR, Phys. Ser.].
[14] I. N. Mikhaĭlov and P. N. Usmanov, Yad. Fiz. **54**, 1239 (1991) [Sov. J. Nucl. Phys. **54**, 753 (1991)].
[15] I. N. Mikhaĭlov, Ch. Briançon, P. N. Usmanov, and É. Kh. Yuldashbaeva, Report R4-85-8, JINR, Dubna (1985) [in Russian].
[16] I. N. Mikhailov, Ch. Briançon, R. L. Whalen *et al.*, Rapport d'Activité CSNSM, 1983–1984, Orsay, France, p. 83.
[17] K. Ya. Gromov, T. A. Islamov, and P. N. Usmanov, Izv. Akad. Nauk SSSR, Ser. Fiz. **53**, 858 (1989) [Bull. Acad. Sci. USSR, Phys. Ser.].
[18] I. N. Mikhaĭlov, P. N. Usmanov, A. A. Okhunov, and Ch. Briançon, Izv. Akad. Nauk SSSR, Ser. Fiz. **56**, 121 (1992) [Bull. Acad. Sci. USSR, Phys. Ser.].
[19] I. N. Mikhaĭlov, P. N. Usmanov, A. A. Okhunov *et al.*, Izv. Russ. Akad. Nauk, Ser. Fiz. **57**, 17 (1993) [Bull. Russ. Acad. Sci., Phys. Ser.].
[20] K. Ya. Gromov, P. N. Usmanov, A. Kh. Kholmatov *et al.*, Yad. Fiz. **56**, No. 12, 29 (1993) [Phys. At. Nucl. **56**, 1635 (1993)].
[21] D. Bohle, A. Richter, W. Steffen *et al.*, Phys. Lett. A **137**, 27 (1984).
[22] D. Bohle, G. Kuchler, A. Richter, and W. Steffen, Phys. Lett. B **148**, 260 (1984).
[23] U. E. P. Berg, C. Blasing, J. Drexler *et al.*, Phys. Lett. B **149**, 59 (1984).
[24] A. Richter, in *Proc. of the Niels Bohr Centennial Conference on Nuclear Structure* (North-Holland, Amsterdam, 1985), p. 469.
[25] J. A. Corr, F. Petrovich, R. J. Philpott *et al.*, Phys. Rev. Lett. **54**, 881 (1985).
[26] C. Djalali, N. Marty, M. Morlet *et al.*, Phys. Lett. B **164**, 269 (1985).
[27] C. Wesselborg, P. Von Brentano, K. O. Zell *et al.*, Phys. Lett. B **207**, 22 (1988).
[28] A. Zilges, P. Von Brentano, C. Wesselborg *et al.*, Nucl. Phys. A **507**, 399 (1990).
[29] A. A. Kuliev and N. I. Pyatov, Yad. Fiz. **20**, 297 (1974) [Sov. J. Nucl. Phys. **20**, 153 (1975)].
[30] T. Suzuki and D. J. Rowe, Nucl. Phys. A **289**, 461 (1977).
[31] V. G. Soloviev, A. V. Sushkov, and N. Yu. Shirikova, Nucl. Phys. A **568**, 244 (1994).
[32] V. G. Soloviev, A. V. Sushkov, and N. Yu. Shirikova, in *Proc. of the Fifth Intern. Spring Seminar on Nuclear Physics: New Perspectives in Nuclear Structure*, Rovello, Italy, May, 1995, p. 340.
[33] F. Iachello, Phys. Rev. Lett. **53**, 1427 (1984).
[34] M. Sambataro, O. Scholten, A. E. L. Dieperink, and G. Piccito, Nucl. Phys. A **423**, 333 (1984).
[35] E. Lipparini and S. Stringari, Phys. Lett. B **130**, 139 (1983).
[36] R. Nojarov and A. Faessler, Z. Phys. A **336**, 151 (1990).
[37] A. Faessler, R. Nojarov, and F. G. Scholtz, Nucl. Phys. A **515**, 237 (1990).
[38] N. Lo Iudice, in *Proc. of the Fourth Intern. Conf. on Selected Topics in Nuclear Structure*, Dubna, Russia, July, 1994, E4-94-168, p. 72.
[39] N. Lo Iudice and F. Palumbo, Phys. Rev. Lett. **41**, 1532 (1978).
[40] G. De Franceschi, F. Palumbo, and N. Lo Iudice, Phys. Rev. C **29**, 1496 (1984).
[41] N. A. Voinova-Eliseeva and I. A. Mitropol'skiĭ, Fiz. Élem. Chastits At. Yadra **17**, 1173 (1986) [Sov. J. Part. Nucl. **17**, 521 (1986)].
[42] L. A. Borisoglebskiĭ, Usp. Fiz. Nauk **81**, 271 (1963) [Sov. Phys. Usp. **6**, 715 (1964)].
[43] J. O. Rasmussen, Nucl. Phys. **19**, 85 (1960).
[44] R. M. Ronningen, R. S. Grantham, J. H. Hamilton *et al.*, Phys. Rev. C **26**, 97 (1982).
[45] R. S. Grantham *et al.*, Bull. Am. Phys. Soc. **20**, 1190 (1975).

[46] F. W. N. De Boer, P. F. A. Goudsmit, P. Koldewich *et al.*, Nucl. Phys. A **169**, 577 (1971).
[47] C. W. Reich and J. E. Cline, Nucl. Phys. A **159**, 181 (1970).
[48] J. E. Cline and C. W. Reich, Phys. Rev. **129**, 2152 (1963).
[49] P. T. Prokof'ev and G. L. Rezvaya, Izv. Akad. Nauk SSSR, Ser. Fiz. **34**, 719 (1970) [Bull. Acad. Sci. USSR, Phys. Ser.].
[50] K. G. Tirsell and L. G. Multhauf, Phys. Rev. C **7**, 2108 (1973).
[51] R. L. West, E. G. Funk, A. Visvanathan *et al.*, Nucl. Phys. A **270**, 300 (1976).
[52] J. M. Domingos, G. D. Symons, and A. C. Douglas, Nucl. Phys. A **180**, 600 (1972).
[53] H. Ikegami *et al.*, Bull. Inst. Chem. Res., Kyoto Univ. **52**, 132 (1974).
[54] K. L. Baker, J. H. Hamilton, J. Lange *et al.*, Phys. Lett. B **57**, 441 (1975).
[55] D. R. Haenni *et al.*, Report ORO-4322-18 (1976).
[56] E. P. Grigor'ev *et al.*, in *Beta Spectrometers and Their Use* [in Russian] (Lithuanian Academy of Sciences, 1974), p. 69.
[57] A. W. Sunyar, Preprint BNL-13530, Brookhaven National Laboratory, Upton, N.Y. (1969).
[58] J. J. Reidy *et al.*, Phys. Rev. B **133**, 556 (1964).
[59] L. M. Quinones, M. Behar, and H. Grobowsky, Bull. Am. Phys. Soc. **18**, 37 (1973).
[60] W. Gelletly, W. F. Davidson, J. Simic *et al.*, J. Phys. G **4**, 575 (1978).
[61] F. K. McGowan, W. T. Milner, R. L. Robinson *et al.*, Nucl. Phys. A **297**, 51 (1978).
[62] A. J. Becker and R. M. Steffen, Phys. Rev. **180**, 1043 (1969).
[63] R. Bengtsson and S. Frauendorf, Nucl. Phys. A **327**, 139 (1979).
[64] Y. El Masri, J. M. Ferte, R. Janssens *et al.*, Nucl. Phys. A **271**, 133 (1976).
[65] A. A. Abdurazakov, Ya. Vrzal, K. Ya. Gromov *et al.*, Izv. Akad. Nauk SSSR, Ser. Fiz. **32**, 749 (1968) [Bull. Acad. Sci. USSR, Phys. Ser.].
[66] N. A. Bonch-Osmolovskaya, Ya. Vrzal, E. P. Grigor'ev *et al.*, Izv. Akad. Nauk SSSR, Ser. Fiz. **32**, 98 (1968) [Bull. Acad. Sci. USSR, Phys. Ser.].
[67] K. Kawade, H. Yamamoto, Y. Ikeda *et al.*, Nucl. Phys. A **279**, 269 (1977).
[68] P. Hungerford, W. D. Hamilton, S. M. Scott, and D. D. Warner, J. Phys. G **6**, 741 (1980).
[69] F. K. McGowan and W. T. Milner, Phys. Rev. C **23**, 1926 (1981).
[70] G. Ch. Madueme, Phys. Rev. C **24**, 894 (1981).
[71] S. N. Khan, R. A. Fox, W. D. Hamilton, and M. Finger, J. Phys. G **1**, 727 (1975).
[72] R. Kalish, B. Herskind, and G. B. Hageman, Phys. Rev. C **8**, 757 (1973).
[73] G. Seiler-Clark, D. Pelte, H. Emling *et al.*, Nucl. Phys. A **399**, 211 (1983).
[74] K. S. Krane, Nucl. Phys. A **377**, 176 (1982).
[75] H. R. Hooper, J. M. Davidson, P. W. Green *et al.*, Phys. Rev. C **15**, 1665 (1977).
[76] A. Backlin, G. Hedin, B. Fogelberg *et al.*, Nucl. Phys. A **380**, 189 (1982).
[77] I. N. Mikhailov and Ph. N. Usmanov, Ann. Phys. (Leipzig) **2**, 239 (1993).
[78] J. Konijn, F. W. N. De Boer, A. Van Poelgeest *et al.*, Nucl. Phys. A **352**, 191 (1981).
[79] H. H. Pitz, U. E. P. Berg, R. D. Heil *et al.*, Nucl. Phys. A **492**, 411 (1989).
[80] V. Bjorn, Acta Univ. Ups. Uppsala Diss. Fac. Sci. No. 22, 1 (1987).
[81] Y. Iwata, J. Phys. Soc. Jpn. **49**, 2114 (1980).
[82] S. H. Sie, D. Ward, J. S. Geiger *et al.*, Nucl. Phys. A **291**, 443 (1977).
[83] H. Yamada, T. Katon, M. Fujioka *et al.*, J. Phys. Soc. Jpn. **41**, 1843 (1976).
[84] V. O. Nesterenko, Ph. N. Usmanov, A. A. Okhunov, and C. Fahlander, J. Phys. G **19**, 1339 (1993).
[85] V. O. Nesterenko, Fiz. Élem. Chastits At. Yadra **24**, 1517 (1993) [Phys. Part. Nucl. **24**, 640 (1993)].
[86] I. N. Mikhaĭlov, P. N. Usmanov, and É. Kh. Yuldashbaeva, Yad. Fiz. **45**, 646 (1987) [Sov. J. Nucl. Phys. **45**, 405 (1987)].
[87] Ch. Briançon, I. N. Mikhaĭlov, and P. N. Usmanov, Fiz. Élem. Chastits At. Yadra **50**, 52 (1989) [Sov. J. Part. Nucl. **50**, 31 (1989)].
[88] H. A. Feshbach, Ann. Phys. (N.Y.) **19**, 287 (1962).
[89] R. Kulessa, Ch. Lauterbach, J. D. Boer *et al.*, Z. Phys. A **334**, 299 (1989).
[90] D. D. Warner, R. F. Casten, and W. F. Davidson, Phys. Rev. C **24**, 1713 (1981).
[91] W. Gelletly, P. Van Isacker, D. D. Warner *et al.*, Phys. Lett. B **191**, 240 (1987).
[92] C. Fahlander and I. Thorslund, Nucl. Phys. A **537**, 183 (1992); I. Thorslund, C. Fahlander, A. Backlin *et al.*, Z. Phys. A **342**, 35 (1992).
[93] A. S. Davydov and G. F. Filippov, Nucl. Phys. **8**, 237 (1958).
[94] A. Faessler, W. Grainer, and R. K. Sheline, Nucl. Phys. **70**, 33 (1965).
[95] A. Arima and F. Iachello, Adv. Nucl. Phys. **13**, 139 (1984).
[96] A. Arima, J. Phys. G **14**, Suppl. No. 88, p. S1.
[97] F. R. Metzger, Phys. Rev. C **13**, 626 (1976).
[98] C. Rangacharyulu, A. Richter, H. J. Wortche, and W. Ziegler, Phys. Rev. C **43**, 949 (1991).
[99] H. J. Riezebos *et al.*, Nucl. Phys. A **465**, 1 (1987).
[100] S. Kuyucak and I. M. Morrison, Phys. Rev. Lett. **58**, 315 (1987).

Translated by Patricia A. Millard